

Screen Printing of Fuel and Oxidant Delivery Plates: A Low Cost Manufacturing Alternative

by

Martin L. Perry
B. Eng., Royal Military College of Canada, 1989

A Thesis Submitted in Partial Fulfillment of the Requirements for the
Degree of

MASTER OF APPLIED SCIENCE

in the Department of Mechanical Engineering

We accept this thesis as conforming to the required standard




Dr. Zuomin Dong, Supervisor (Department of Mechanical Engineering)



Dr. Xianguo Li, Department Member (Department of Mechanical Engineering)



Dr. Ron Podhorodeski, Department Member (Department of Mechanical Engineering)



Dr. Keith Prater, External Examiner (Ballard Power Systems)

© Martin L Perry, 1997
University of Victoria

All rights reserved. This thesis may not be reproduced in whole or in part, by photocopy
or other means, without the permission of the author

Abstract


If the premise is accepted that the fuel cell is the next generation transformer technology for the motive industry, then the development of such a technology must be advanced to the point that it becomes a viable both physically and economically. That is not to say that a fuel cell system must achieve the same cost targets as those of the internal combustion engine, rather the new technology must present itself as an economically viable alternative when issues like the environment are taken into account. Determining the cost that the market and environment will bear is up to the economist and environmentalist. Bringing the cost of manufacture for the fuel cell down to the lowest possible level is the responsibility of the engineers, and as such formed the basis of my thesis.

As it stands, the cost of several key fuel cell components must be reduced. The bi-polar plate is one component that has a significant contribution to the overall system cost and also has the greatest potential to be reduced. When considering how to reduce the cost of bi-polar plate manufacturing, several issues were considered. The manufacturing process and the material costs are the two largest contributors to the overall cost. Material costs are insignificant when compared to manufacturing costs, leading to the conclusion that it must be the process that undergoes the development. Traditional plate manufacturing techniques apply a sculpturing approach, where a CNC milling machine is used to cut out the fuel and oxidant delivery channels. A unique and novel approach to the task is to build up the required channel thickness rather than sculpt the material away. Several possibilities exist that may perform the building up task, of which screen printing is the most promising.

The initial goals stipulated that the screen printing process was had to be capable of printing an electrically conductive material onto a suitable substrate to the height of 0.7 mm. When compared with current CNC milled flow field plate manufacturing techniques, the screen printing process developed exhibits the following desirable features: low manufacturing and capital costs, the ability to rapid prototype, flexibility in flow channel design and material properties, mass and batch production capability and little material wastage.

Investigation into conductivity issues of the inks revealed that investigations into the microstructure and percolation theory proved valuable when trying to formulate a ink as conductive as possible. Future work in the area of ink conductivity is recommended.

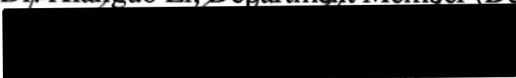
Screen printing techniques were applied and developed to the problem and successfully met the requirements outlined at the beginning of the project. Fuel and oxidant delivery plates were successfully printed and at a considerable cost savings over the CNC milling approach.




Dr. Zuomin Dong, Supervisor (Department of Mechanical Engineering)



Dr. Xianguo Li, Department Member (Department of Mechanical Engineering)



Dr. Ron Podhorodeski, Department Member (Department of Mechanical Engineering)



Dr. Keith Prater, External Examiner (Ballard Power Systems)

Table of Contents

ABSTRACT	II
TABLE OF CONTENTS	IV
LIST OF TABLES	VI
LIST OF FIGURES	VII
NOMENCLATURE	VIII
ACKNOWLEDGEMENTS	IX
CHAPTER 1	1
1. INTRODUCTION	1
1.1 MOTIVATION - FUEL CELLS FOR TRANSPORTATION.....	1
1.2 THE FUEL CELL.....	8
1.2.1 <i>What it is</i>	8
1.2.2 <i>Theory of Fuel Cells</i>	10
1.2.3 <i>Fuel Cell Characterization</i>	11
1.3 FUEL CELLS FOR TRANSPORTATION.....	12
1.3.1 <i>Fuel cell versus IC engine</i>	12
1.3.2 <i>PEM Fuel Cell - The Transportation Choice</i>	14
1.3.3 <i>PEM Fuel Cell Components</i>	15
1.3.3.1 MEA.....	16
1.3.3.2 Bi-Polar Plate.....	17
1.4 THESIS OBJECTIVES.....	19
1.5 THESIS APPROACH.....	20
CHAPTER 2	22
2. SCREEN PRINTING-STATE OF THE ART	22
2.1 HISTORY OF SCREEN PRINTING.....	22
2.2 EQUIPMENT.....	24
2.2.1 <i>Screen Mesh</i>	24
2.2.2 <i>Screen Mesh Materials</i>	27
2.2.3 <i>Frame</i>	29
2.2.4 <i>Stencils</i>	30
2.2.5 <i>Squeegee</i>	32
2.3 INKS.....	34
2.4 PRINTING MACHINERY AND TECHNIQUES.....	37

CHAPTER 3	43
3. SCREEN PRINTING APPLIED TO MANUFACTURING OF FLOW FIELD PLATES	43
3.1 MOTIVATION FOR USING SCREEN PRINTING.....	43
3.2 TECHNICAL REQUIREMENTS AND OBJECTIVES	46
3.3 MATERIAL SELECTION.....	48
3.3.1 Ink Base	48
3.3.2 Printing Substrate	49
3.3.3 Conductive Filler Material	51
 CHAPTER 4	 53
4. PRINTING TECHNIQUES AND INK DEVELOPMENT.....	53
4.1 THE EVOLUTION OF THICK DEPOSIT PRINTING TECHNIQUE.....	53
4.2 INK DEVELOPMENT	65
4.2.1 Conductivity	67
4.2.1.1 Conductivity Results.....	70
4.2.2 Microstructure	74
4.2.2.1 Percolation Theory.....	76
4.2.3 Cost Analysis.....	78
4.2.3.1 Material Costs.....	79
4.2.3.2 Process Cost.....	80
 CHAPTER 5	 81
5. CONCLUSIONS AND FUTURE WORK.....	81
5.1 CONCLUSIONS.....	81
5.1.1 Process Feasibility	81
5.1.2 Ink Conductivity and New Research Directions	82
5.2 FUTURE WORK AND RECOMMENDATIONS.....	84
5.2.1 Screen Printing.....	85
5.2.2 Ink Conductivity.....	86
 REFERENCES.....	 88
 APPENDIX A.....	 91
Van der Pauw Resistivity Circuitry Layout.....	91

List of Tables

TABLE 1.1: CARB EMISSION STANDARDS FOR LIGHT DUTY VEHICLE; NMOG = NON-METHANE ORGANIC GASES; NMHC = NON-METHANE HYDROCARBONS; TLEV = TRANSITIONAL LOW EMISSION VEHICLE; LEV = LOW EMISSION VEHICLE; ULEV = ULTRA LOW EMISSION VEHICLE.....	7
TABLE 1.2: CARB MINIMUM PHASE-IN SCHEDULE (UP TO YEAR 2000) FOR LIGHT-DUTY VEHICLES; ZEV = ZERO EMISSION VEHICLE.....	7
TABLE 1.3: FUEL CELL TYPES AND PROPERTIES.....	14
TABLE 5.1: HUMIDITY TEST CHAMBER MATERIALS AND RESULTS.....	67
TABLE 5.2: CONDUCTIVE INK MIXTURES TESTED.....	70
TABLE 5.3: SAMPLE RESISTIVITY RESULTS	72
TABLE 5.4: CRITICAL AREA FRACTION AS A FUNCTION OF ASPECT RATIO.....	78
TABLE 5.5: UNION CARBIDE GRAFOIL PREMIUM NUCLEAR GRADE RETAIL PRICE QUOTES.....	79

List of Figures

FIGURE 1.1: CARBON DIOXIDE EMISSIONS IN BRITISH COLUMBIA	3
FIGURE 1.2: CARBON MONOXIDE EMISSIONS IN BRITISH COLUMBIA.....	4
FIGURE 1.3: VOLATILE ORGANIC COMPOUND EMISSIONS IN BRITISH COLUMBIA.....	4
FIGURE 1.4: SOURCES OF NITROGEN OXIDES IN BRITISH COLUMBIA	5
FIGURE 1.5: FINE PARTICULATE CONTAMINATION SOURCES FOR BRITISH COLUMBIA.....	6
FIGURE 1.6: A TYPICAL FUEL CELL CONFIGURATION.....	9
FIGURE 1.7: CHEMICAL STRUCTURE OF DUPONT'S NAFION AND DOW'S PERFLUOROSULPHONATE IONOMER MEMBRANES.....	16
FIGURE 3.1: TYPICAL SCREEN PRINTING APPARATUS	24
FIGURE 3.2: SCREEN MESH THICKNESS VS. PRINT THICKNESS	26
FIGURE 3.3: THE EFFECTS OF LIGHT SCATTER. COLOURED SCREEN MESH ABSORBS ACTINIC UV RADIATION.....	28
FIGURE 3.4: INK FLOW AS A FUNCTION OF SQUEEGEE ANGLE.....	33
FIGURE 3.5: SQUEEGEE BLADE TYPES.....	33
FIGURE 3.6: TYPICAL HAND-BENCH PRINTING SET-UP	37
FIGURE 3.7: PRINCIPLE OF OFF-CONTACT ADJUSTMENT.....	39
FIGURE 3.8: COMMON PRINTING MACHINE ARRANGEMENTS	40
FIGURE 5.1: PRINTING APPARATUS CONSTRUCTED	58
FIGURE 5.2: THE FLOODING PRINCIPLE.....	60
FIGURE 5.3: DEPOSITION THICKNESS THEORY ILLUSTRATION	61
FIGURE 5.4: SQUEEGEE PULL AND STENCIL ANGLE RELATIONSHIP.....	64
FIGURE 5.5: CONDUCTIVE INK OPTIONS.....	68
FIGURE 5.6: VAN DER PAUW CORRECTION FACTOR f	69
FIGURE 5.7: CONFOCAL MICROSCOPE PICTURES OF (A) 30 WEIGHT PERCENT GRAPHITE, 53-75M PARTICLE SIZE IN WB5101 (B) 30 WEIGHT PERCENT GRAPHITE, <53 M PARTICLE SIZE IN WB5101	75
FIGURE 5.8: UNIVERSAL SHAPE OF THE RESISTIVITY VERSUS FILLER LOADING PLOT.....	77
FIGURE 5.9: SCREEN PRINTING BI-POLAR PLATE PROCESS CONFIGURATION.....	80

Nomenclature

μ^a	Chemical potential at the anode
μ^c	Chemical potential at the cathode
G	Gibbs free energy
eV	Electron volts
$-q_e$	Electron charge

Acknowledgements

First and foremost, I would like to thank Dr. David Sandborn Scott for planting the fuel cell seed in my brain during one of his energy systems lectures. His inspiration motivated me to change the path of my master's program and my life. I would also like to thank Dr. Zuomin Dong, my supervisor, for giving me the opportunity to work with the TERS fuel cell team and also for providing words of wisdom, encouragement, and unfaltering confidence.

A major influence as to the success of this thesis was made by my colleagues Pat George and George Thiessen of the Department of Visual Arts at the University of Victoria. Their support and knowledge were instrumental in the development of the printing technique. I appreciate their patience and tolerance of the engineering way of doing things.

I would like to thank the whole group at IESVic including fellow graduate students, project engineers and support staff. I am grateful for their patience, words of encouragement and belief in some not so believable ideas. The support received by Ballard and especially Keith Prater must also be acknowledged as a significant contribution to the success of this thesis. I am grateful for the research opportunity made possible by funding from NSERC and BG plc.

Finally, I wish to thank my friends and family for their support, patience and encouragement. I would especially like to thank Michelle for putting up with my sometimes bizarre work patterns and my newly born child, Emma, for motivating me to get as much of my thesis done after her arrival in this world and not letting me linger in the world of graduate limbo.

Chapter 1

1. Introduction

1.1 Motivation - Fuel Cells for Transportation

The combustion of fossil fuels is the most heavily relied upon transformation technology for power generation, heating and transportation [1]. The World's energy system will continue to rely primarily on fossil fuels, at least through 2020, and is unlikely to suffer major stresses affecting its sustainability or security [6]. This same technology is also considered the greatest contributor to global warming, environmental degradation and human health risks [6]. For these reasons the search for alternatives to the use of fossil fuels has become a focus of a large number of people.

When a fossil fuel is burned, the carbon it contains is combined with oxygen in the air, to release heat. The combustion process also produces byproducts, many of which are potentially harmful and are known as air pollutants. Among the list of combustion products, those of major concern are: carbon dioxide (CO_2), carbon monoxide (CO), volatile organic compounds (VOCs), nitrogen oxides (NO_x), sulphur oxides (SO_x), and very fine particulates. In addition unburned hydrocarbons, some of which evaporate directly from the gas tanks of cars and trucks, escape before and after combustion and join other VOCs in the air.

Carbon dioxide is an odourless, colourless gas that is attributed with adversely affecting the earth's weather system by causing a gradual warming trend around the globe, thus altering ocean currents, precipitation patterns, the global climate and all living things.

This phenomenon is known as the enhanced greenhouse effect. Carbon dioxide levels in the atmosphere have reached concentrations that are more than 25 percent higher than at any levels found in the 220,000 years of the earth's recorded atmospheric history [5]. The average world temperature is 4 to 6 degrees warmer than the last ice age and that, if continued on the same path, they will rise a further 1 to 4 degrees within the next century [5]. Of the rise in temperature for the last century over half of that increase has occurred in the last 20 years [5]. Night time temperatures are rising up to three times faster than daytime temperatures [5]. Globally the 10 warmest years on record have occurred since 1980. Over the last 63 seasons, 42 were warmer than normal and 44 were wetter than normal. Over the last four years there have been three El Niños - unprecedented in the last 50 years [5].

Although these statistics point to the obvious, harmful emissions must be reduced some countries and governments continue to ignore these needs to further their economic gain. Industrialized countries must lead the way in searching for alternate transformer technologies and developing them to the point that they become an economic and technically viable alternative to the use of fossil fuels. One sector of the energy consuming market, transportation, has a challenging task ahead.

Amongst the sources of air pollution, the transportation sector is increasing its contribution to the overall total. California, in the United States, is leading the way in the development and implementation of clean air legislation by necessity. In recent years they have pushed for and adopted strict emission control regulations pertaining to all passenger vehicles and also the light truck market. Locally, in British Columbia, air pollution is becoming an increasing concern of the environmentalist, but little is being done in terms of legislation when compared with California. However with the large influx of inhabitants to

the Lower Fraser Valley area in recent years and the increased number of vehicles plying the highways every day, vehicular pollution will soon gain a prominent position.

In British Columbia the largest single source of the pollution problem is the transportation sector. Provincially transportation accounts for: 49 percent of carbon dioxide emissions, 50 percent of nitrogen oxide emissions, 34 percent of carbon monoxide emissions, 30 percent of hydrocarbon emissions, and 9 percent of particulate emissions [5]. In the United States, about 81 percent of the air emissions (1986) were from the transportation segment which also accounts for over 60 percent of petroleum usage [9]. Figure 1.1 illustrates the contribution transportation is making to the carbon dioxide pollution problem in British Columbia [7].

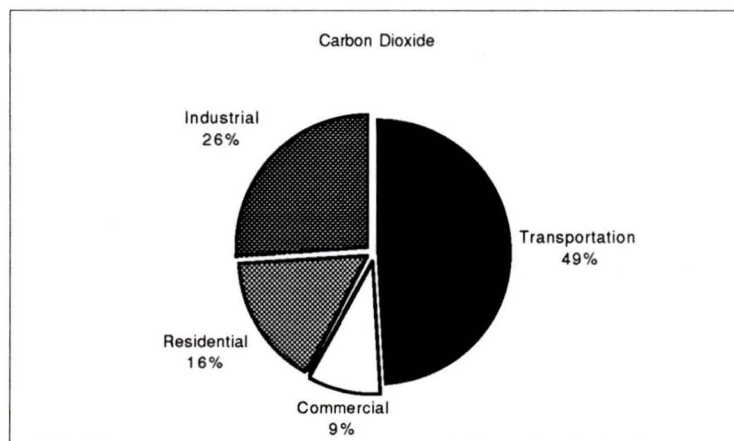


Figure 1.1: Carbon Dioxide Emissions in British Columbia

Carbon monoxide, at high concentrations, can pose acute health risks since the body can become starved for oxygen when the gas is inhaled and absorbed into the bloodstream. Concentrations of 0.1 percent can cause death, while lower concentrations may impair perception and reflexes [7]. Carbon monoxide also inadvertently adds to the greenhouse effect by interfering with the natural breakdown of methane, a greenhouse gas. Figure 1.2 illustrates the contribution to the carbon monoxide pollution problem that the transportation sector is responsible for [7].

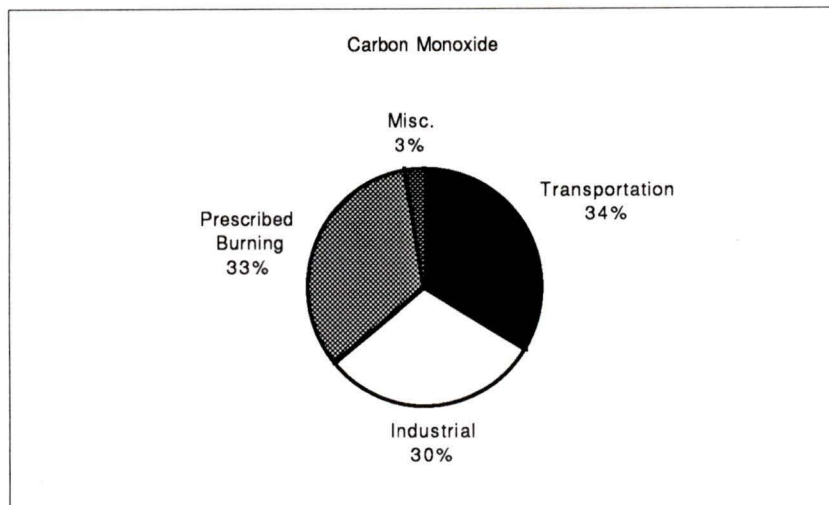


Figure 1.2: Carbon Monoxide Emissions in British Columbia

Volatile organic compounds are substances that originate in plant matter and evaporate readily at ordinary pressures and temperatures. By far the greatest source of VOCs is vegetation, but the greatest source from human activity is from transportation [7]. Hydrocarbons, one group within the VOC family, are prime components of fuels such as methane, propane, natural gas, gasoline and kerosene. VOCs also contribute to the formation of ground-level ozone which poses a health hazard. Figure 1.3 illustrates the contribution to VOCs made by various producers in British Columbia [7].

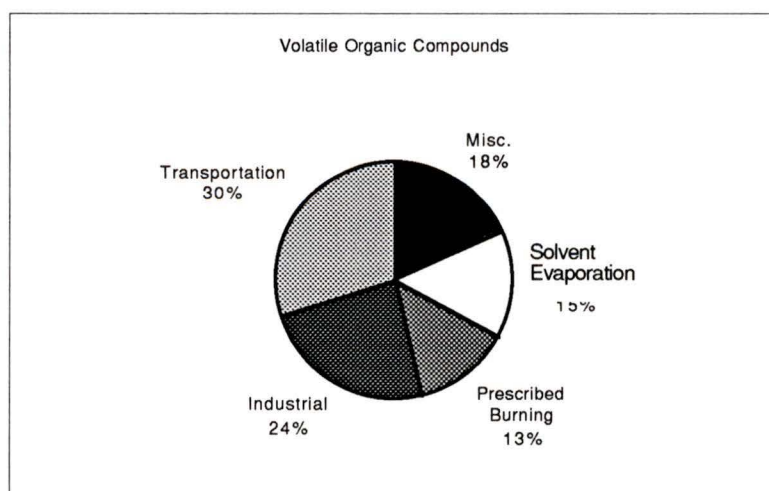


Figure 1.3: Volatile Organic Compound Emissions in British Columbia

Nitrogen dioxide can reduce atmospheric visibility with a distinctive brown haze. Both nitrogen dioxide and sulphur dioxide can increase susceptibility to respiratory infection and airway constriction in those with asthma. Both gases are altered in the atmosphere to become fine particulates in the form of sulphates and nitrates, or acid rain when combined with water. Acidic contamination can affect human health directly when inhaled, and indirectly when they fall on surface water, land and plants. Figure 1.4 reveals the sources of nitrogen oxides as found in British Columbia [7].

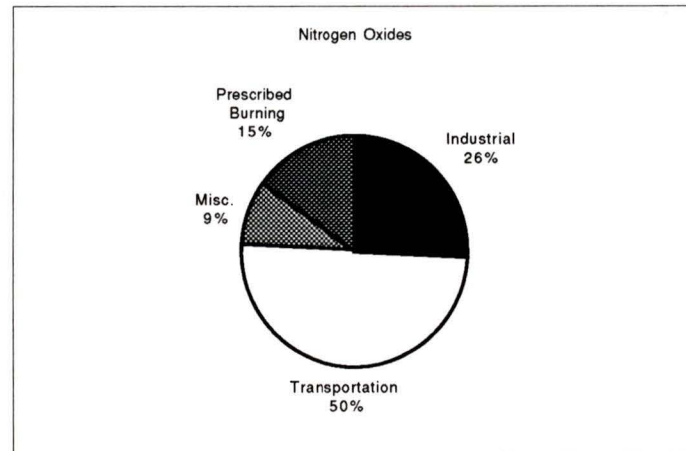


Figure 1.4: Sources of Nitrogen Oxides in British Columbia

Fine particulates are particles so small they remain suspended in the air where they can be inhaled and deposited deep in the respiratory system. Primary fine particulates are released directly into the air from sources such as tailpipes. Secondary fine particulates are formed from physical and chemical reactions involving gases such as NO_x , SO_x , and VOCs, emitted into the air. PM_{10} refers to particles that are 10 microns or less in diameter. $\text{PM}_{2.5}$ refers to very fine particles that are 2.5 microns or less in diameter. Secondary particulates are made up primarily of $\text{PM}_{2.5}$. In the Lower Fraser valley, diesel and gasoline vehicles are thought to be the major source of $\text{PM}_{2.5}$ [7]. Diesel engines, while less than 10 percent of the total vehicle fleet, contribute more than 40 percent of the

transportation related particulate emissions [7]. Figure 1.5 illustrates the sources of fine particulate contamination in British Columbia [7].

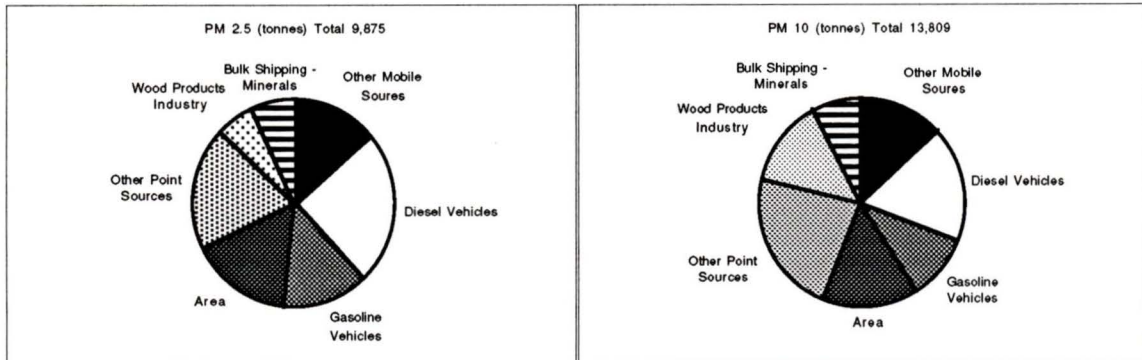


Figure 1.5: Fine Particulate Contamination Sources for British Columbia

Health impacts of poor air quality range from irritation of the eyes, nose and respiratory tract to more serious problems such as impaired lung function, decreased resistance to infection, increased incidence and severity of asthmatic attacks, lung cancer, reproductive problems, birth defects, and premature death mainly due to respiratory and heart conditions [7]. In addition air pollution reduces crop yields, damages forests and other vegetation, destroys building materials, impairs visibility and spoils the natural beauty of our planet.

As stated previously, the adoption of low emission transformer technology legislation is increasing, especially in areas greatly affected by the vehicle emission pollution problem. California has recently begun to legislate the use of lower polluting alternative fuels. The California Air Resource Board (CARB) has set standards for tailpipe emissions and had legislation passed that mandates conversion of vehicles that meet the progressively stringent standards. The Environmental Protection Agency has recently recommended that the CARB legislation be adopted by all other states as a standard urban pollution abatement policy [3]. Table 1.1 shows the CARB emission standards for light duty vehicles [4].

Table 1.1: CARB emission standards for light duty vehicle; NMOG = non-methane organic gases; NMHC = non-methane hydrocarbons; TLEV = transitional low emission vehicle; LEV = low emission vehicle; ULEV = ultra low emission vehicle

Pollutant	Grams per Mile		
	TLEV	LEV	ULEV
NMOG	0.125	0.075	0.04
CO	3.4	3.4	1.7
NO _x	0.4	0.2	0.2
Formaldehyde	0.015	0.015	0.008

Table 1.2 shows the mandated conversion schedule for light-duty vehicles specified by CARB [4].

Table 1.2: CARB minimum phase-in schedule (up to year 2000) for light-duty vehicles; ZEV = zero emission vehicle

Model Year	TLEV	LEV	ULEV	ZEV
1994	10 percent			
1995	15 percent			
1996	20 percent			
1997		25 percent	2 percent	
1998		48 percent	2 percent	2 percent
1999		73 percent	2 percent	2 percent
2000		96 percent	2 percent	2 percent

To achieve the goals outlined in this legislation, and others like it, is a major feat but definitely a step in the right direction. Several technologies present themselves as contenders for the various CARB stages, but the one transformer technology that is a

contender for fulfilling all the requirements outlined above is the Proton Exchange Membrane (PEM) fuel cell.

1.2 The Fuel Cell

1.2.1 What It Is

A fuel cell can be defined as an electrochemical device which can continuously convert the chemical energy in a reducing agent and an oxidant fuel to electrical energy by a process involving an electrode electrolyte system [8]. Unlike an electric cell or battery, a fuel cell does not run down or require charging; it operates as long as the fuel and an oxidizer are supplied continuously from outside the cell.

A fuel cell is typically made up of three components: an anode to which the fuel is supplied, a cathode, to which an oxidant is supplied, and an electrolyte, which permits the flow of ions (but not electrons or reactants) between the anode and the cathode. Figure 1.6 illustrates a typical fuel cell configuration [1].

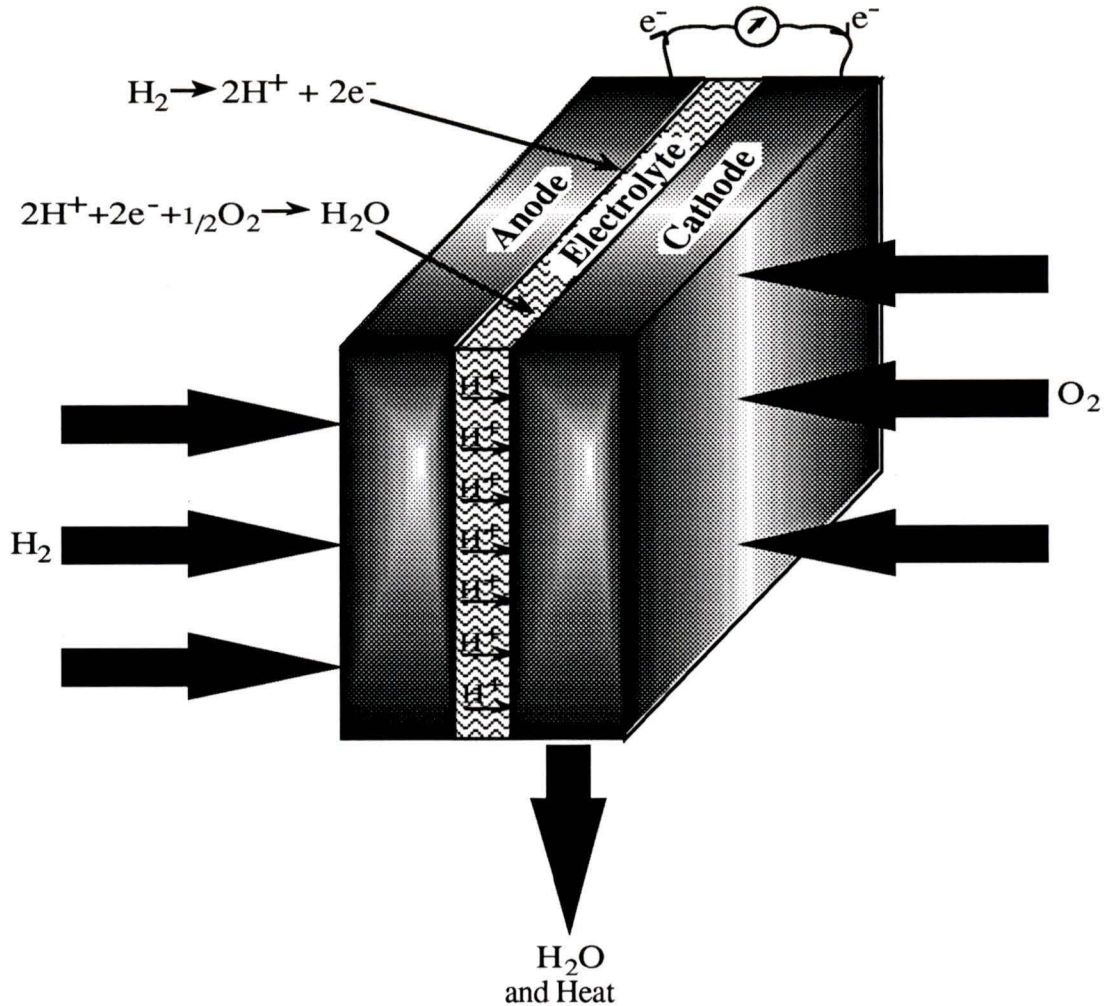


Figure 1.6: A Typical Fuel Cell Configuration

This typical fuel cell consumes reactants and generates a current. The reactants, hydrogen and oxygen in this case, move to the electrolyte through rough-surfaced, porous, electrically conductive electrodes. Electrons are produced at the anode-electrode interface, pass through an external circuit and are then consumed at the cathode-electrolyte interface. Besides electrical power, the fuel cell also generates useable water and heat. A typical fuel cell voltage is about one volt. The anode of one cell is connected electrically to the cathode of another creating a series circuit thereby increasing the voltage. The required unit voltage is achieved by combining cells into a stack.

1.2.2 Theory of Fuel Cells

Most fuel cells being developed consume either hydrogen or fuels that have been preprocessed into a suitable hydrogen-rich form. Some fuel cells can directly consume sufficiently reactive fuels such as methane, methanol, carbon monoxide or ammonia, or can process such fuels through an internal reformer. For the purpose of brevity this section will deal with hydrogen as the fuel.

At the anode the hydrogen molecules dissociate into H^+ ions, which are free to migrate across the electrolyte toward the cathode, and electrons, which are free to pass through the external load. This dissociation occurs spontaneously since there is an equilibrium ratio of hydrogen molecules and ions:



At the cathode, oxygen molecules similarly dissociate into atoms, which combine with electrons and the migrating H^+ ions to form water:



An electric potential appears between the electrodes because of the excess of electrons at the anode, where they are generated, compared with the cathode, where they are consumed. It is this potential that forces the current to flow through the external circuit.

To derive the magnitude of the electric potential across the electrodes, the chemical potential of the system is considered. With an open circuit, no current is flowing, and the partial reactions occurring at the anode and the cathode are at equilibrium. By definition, equilibrium exists when the chemical potential of the products equals that of the reactants, so:

$$\mu^a(H_2) = 2\mu^a(H^+) + 2\mu^a(e^-) \quad (1.3)$$

and,

$$\mu^c(\text{H}_2\text{O}) = 2\mu^c(\text{H}^+) + 2\mu^c(\text{e}^-) + \frac{1}{2}\mu^c(\text{O}_2) \quad (1.4)$$

where μ^a and μ^c are the chemical potentials at the anode and cathode respectively. Since the ionic charge carriers can migrate freely through the electrolyte, the chemical potentials of the ions at the two electrodes are also at equilibrium:

$$\mu^a(\text{H}^+) = \mu^c(\text{H}^+) \quad (1.5)$$

The voltage difference that appears between the two electrodes is a factor of their different electrochemical potentials:

$$\mathbf{V} \equiv [\mu^c(\text{e}^-) - \mu^a(\text{e}^-)]/q_e \quad (1.6)$$

where $-q_e$ is the electron's charge. The above three equilibrium conditions yield the total work provided by the fuel cell:

$$\mathbf{W} = -2q_e \mathbf{V} = -[\mu^c(\text{H}_2\text{O}) - \frac{1}{2}\mu^c(\text{O}_2) - \mu^a(\text{H}_2)] = -\Delta\mathbf{G} \quad (1.7)$$

where $-\Delta\mathbf{G}$ is the change in Gibbs free energy for the formation of a water molecule. (Note the factor $2q_e$ arises because two electrons are transferred per water molecule formed.)

In this particular case, the potential difference is 1.23 V, and the work done per molecule of water produced is 2.46 eV. As stated earlier, a practical system uses a stack of many fuel cells with the anode of one cell in electrical contact with the cathode of the adjacent cell, resulting in a series summing of the cells potential differences.

1.2.3 Fuel Cell Characterization

Different types of fuel cells are characterized by the different ions used to carry charge across the electrolyte from one electrode to the other. Fuel cells that use acidic electrolytes, such as phosphoric acid or proton exchange membrane (PEM) fuel cells, rely on the proton, H^+ , to carry the charge from the anode to the cathode. In other fuel cells

the charge is carried from the cathode to the anode via $O^=$ ions, as found in solid oxide ceramic fuel cells, OH^- ions found in alkali fuel cells, and $CO_3^=$ ions of the molten carbonate type fuel cells.

1.3 Fuel Cells for Transportation

1.3.1 Fuel Cell versus IC Engine

The internal combustion (IC) engine has undergone nearly a century of development since its invention. At present the IC engine is the primary energy conversion technology being employed with regards to the terrestrial transportation market. The fuel cell, although the concept was first introduced in 1839 by Sir William Grove, has undergone relatively little development. The amount of R&D spent on fuel cells is a disproportionately small part of total energy R&D in almost all countries [9]. The last thirty years, however, have witnessed a renewed enthusiasm towards the fuel cell. The industries which have exhibited the most influence on fuel cell development have been the defence industry, space and extraterrestrial vehicle developers, and stationary power developers [9].

Each of these applications had extraneous conditions that permitted the high cost of fuel cell technology to be disregarded in favour of the fuel cells neat technology. The adoption of fuel cells into other niche markets however requires the cost of the technology to be greatly reduced. It will be difficult for fuel cells to compete with internal combustion engines on an initial cost basis. An IC engine and transmission, for example, producing 500 W/kg costs about \$15 /kg or \$30 /kW [10]. In the automotive industry the fuel cell must be available at a cost of \$150 /kW while the truck and bus markets demand a price

less than \$300 /kW for it to be competitive with current IC technology [9]. At present these cost targets are far from being achieved, but the potential exists.

The cost is not the only ground by which the rival technologies can be compared. In terms of power density the two technologies are much closer. Recent PEM fuel cell developments by Ballard have seen a six fold increase in power density in just three years (Ballard MK V, 5 kW air, 169 W/kg 1992; Ballard 1000 W/kg, Nov. 95). The typical IC automobile engine and transmission produces 500 W/kg, indicating that the fuel cell is more than capable of achieving the automobile power requirements [10]. The bus and truck markets are more demanding in terms of power requirements, but Ballard's tests of their fuel cell powered zero emission bus indicate that these demands have also been satisfied. These results, for the bus application, translate into performances comparable to the present diesel plants being used in terms of acceleration and fuel economy. Future development will more than likely push the fuel cell beyond the current diesel capabilities.

The minimal maintenance required of the fuel cell plant when compared with the IC engine will present itself as a positive selling feature. The lack of moving parts in the fuel cell mean that mechanical failure due to wear is eliminated. The expected life span of future PEM fuel cell systems is over 40,000 hours [9][10]. This durability translates into the "engine" far outlasting the remainder of the vehicle components.

Fuel cells are also attractive alternatives when considering the pollution issue. Under the category of vehicle emissions, the fuel cell proves itself to be the unquestionable winner. The fuel cell that runs on hydrogen produces zero harmful emissions. Section 1.1 of this chapter was dedicated to the environmental impact of hydrocarbon based fuels as used in the IC engine. Its length indicates the vast separation that exists between the two transformer technologies and the need for the development of alternative technologies like

the fuel cell. The cost difference of the technologies may eventually carry less weight when the state of the environment and hidden health care costs are recognized and considered. The fuel cell coupled with an electric drive train would also result in a substantially quieter vehicle, thus reducing overall noise pollution along major traffic corridors.

1.3.2 PEM Fuel Cell - The Transportation Choice

Each particular market requires a specific set of fuel cell characteristics. The most common criteria that fuel cells are assessed by include (i) fuel efficiency; (ii) power density, which is important from the points of view of minimizing weight, volume, and capital costs of the plant; (iii) projected rated power level; (iv) projected lifetime, and; projected capital costs [9]. Table 1.3 illustrates the various fuel cell types and their individual ratings on the above criteria [9].

Table 1.3: Fuel Cell Types and Properties.

Type of fuel cell and of fuel	Power Density (mWcm ⁻²)		Rated Power level projected (kW)	Lifetime projected (h)	Capital costs projected (\$/kW)	Applications, time frame
	Present	Projected				
Alkaline, H ₂	100-200	>300	10-100	>10,000	>200	Space 1960- Transportation 1996- Standby power 1966-
Phosphoric Acid, CH ₄ , CH ₃ OH	200	250	100-5000	>40,000	1000-	Onsite integrated energy systems peak sharing
Molten Carbonate, CH ₄ , coal	100	200	1000-100,000	>40,000	1000	Base load and intermediate load power generation, cogeneration 1996-
Solid Oxide, CH ₄ , coal	240	300	100-100,000	>40,000	1500	Base load and intermediate load power generation, cogeneration 2000-, Space and terrestrial
Solid polymer H ₂ , CH ₃ OH	350	>600	1-1000	>40,000	>200	Space 1960-, transportation 1996-, Standby power 1992-, Underwater 1996-
Direct methanol CH ₃ O + 1	40	>100	1-100	>10,000	>200	Transportation 2010- Remote power 2000-

Molten Carbonate Fuel Cells (MCFC) and Solid Oxide Fuel Cells (SOFC) are clearly targeted for large stationary utility applications where the high operating temperatures (600°C and 1000°C respectively) can be accommodated and are in fact useful. From Table 1.3 above, the three fuel cell types that are contenders for the

transportation industry are the alkaline, the solid polymer or PEM, and the direct methanol fuel cells. A PEM fuel cell is the only realistic fuel cell choice for an alternative motive application [20]. The Alkaline Fuel Cell (AFC) has mainly been used in the aerospace industry where oxygen is used. The AFC electrolyte deteriorates from the carbon dioxide present in ambient air. Phosphoric Acid Fuel Cells (PAFC) are the only other possible choice. Of all other systems it is the most developed, but the PEM fuel cell is superior in this application for the following reasons [20]:

- PEM fuel cell has higher power density; this results in an acceptable weight and volume; the power plant will be compact.
- PEM operates at 70°C to 80°C (the lowest of any fuel cell type) which allows immediate startup; this low temperature makes it safe for operators and users.
- PEM electrolyte is a solid plastic material which results in simpler, more reliable and easier to maintain “engine”; there are no corrosive liquids to handle or leak, and it is operationally forgiving because pressure balances are not critical.
- PEM fuel cells can reach competitive cost targets for alternative motive applications.

For these reasons it is generally accepted in the fuel cell community that the PEM fuel cell has the best chance at dethroning the internal combustion engine from its long reign as the best transformer technology for use in terrestrial based transportation.

1.3.3 PEM Fuel Cell Components

As stated earlier the barrier that presently holds the acceptance of the PEM fuel cell back in terms of the transportation market is its per kilowatt cost. Current production and material costs culminate in a price of approximately \$2000-\$4000 /kW [9]. The high cost can be broken down into three major contributors: the membrane electrode assembly (MEA), the bi-polar plate, and the fuel cell sub-systems or ancillaries. The relative cost of

the ancillaries are more or less fixed. Reduction of these costs depends on new fuel cell configurations that reduce the need for these ancillaries. The two components that have the potential for cost reduction are the MEA and the bi-polar plates [26].

1.3.3.1 MEA

The MEA is one of the key components of the PEM fuel cell. As the name suggests it is made up of two components, the membrane sandwiched between two catalyzed electrodes. The membrane's primary function is to permit proton transport from the anode to the cathode. It must also possess the following desirable properties: high oxygen solubility, high chemical stability, low density, and high mechanical strength. Recent polymeric developments by DuPont and Dow Chemical have replaced the conventional sulphonic acids of polyvinylbenzene-styrene based copolymers. The polymeric electrolyte is completely fluorinated and rides on a polytetrafluoroethylene (Teflon) backbone. The fluorocarbon chain is connected by means of an ether linkage to a sulphonic acid group as illustrated in Figure 1.7 [10].

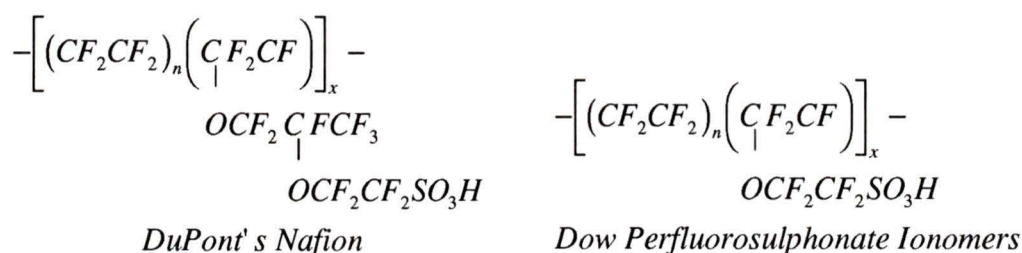


Figure 1.7: Chemical Structure of DuPont's Nafion and Dow's Perfluorosulphonate Ionomer Membranes

The gas-diffusion electrodes that complete the MEA sandwich assembly are typically constructed of a carbon backing (either cloth or paper) and an electrocatalyst. Platinum serves as the electrocatalyst, either supported or not (supported on carbon), and is typically mixed with a Teflon emulsion to bond onto the carbon backing. Platinum loading of 0.4 mg/cm² are typical [2].

The challenge faced by the MEA manufacturers is the reduction of the costs of the proton-conducting membranes and the platinum-catalyzed electrodes. With recent progress in the increase of power densities with low platinum loaded electrodes, the cost of the platinum is about \$30-\$40 /kW [9]. The membranes typically cost \$60-\$200 /kW [9]. The result is a bill for the MEAs between \$500 and \$1250 for a 5 kW stack. In order for the fuel cell to become economically viable, the cost of the MEA is required to be reduced by a factor of 10 to 20 [9].

1.3.3.2 Bi-Polar Plate

The bi-polar plate serves a number of purposes in the fuel cell stack. The plate's primary functions are to: separate the cells of the stack, be electrically conducting, be fitted with flow channels to distribute the fuel and oxidant, be corrosion resistant, and be of low permeability to safely separate H₂ and O₂ feed streams.

Ballard Power Systems, the world leader in PEM fuel cell technology, currently uses a high density graphite plate to function in their bi-polar arrangement. The stock plate is purchased from an external supplier with two of the key acceptance criteria being hydrogen impermeability and surface finish tolerancing to provide an adequate sealing surface [17]. The cost of these plates is approximately \$30 /plate, with one third of that cost associated with the raw material and the further two thirds associated with preprocessing costs mentioned above [17]. After arrival at Ballard the plates are then CNC milled to the desired flow channel patterns. The CNC milling of the plates is a time and labour intensive process with the loading and tolerancing checks performed by hand as well as the sharpening and replacement of the milling bits. Frequent mill bit changes are required due to the poor machinability of the graphite.

At the end of this lengthy process the single unit cost is in excess of \$100 /plate [17]. On the MK V 5 kW stack there are a total of 52 plates which translates into a cost of \$5200 for the stack or \$1040 /kW. The bi-polar plate constitutes approximately one-third of the overall fuel cell cost [17]. As such a reduction in the cost of manufacturing of the bi-polar plate would contribute significantly to the overall lowering of the fuel cell cost.

Several other bi-polar plate manufacturing techniques have been attempted over the last decade with varied results. Some of those methods include the use of molded composites, plastic injection molding, and pressing. In the molded composite and plastic injection molding processes similar problems have plagued their adoption. The primary drawbacks are their low conductivity and high initial cost of production. Several attempts have been made to increase the conductivity by the inclusion of conductive fillers, but the quantities required to achieve adequate conductance introduced problems with mold release and high tool wear. As the thickness of the bi-polar plate decreases the tolerancing required in the mold are more critical, and as of yet the molding process has been unable to satisfy these requirements [17].

An alternative to molding is the pressing technique. In this process a set of dies are made to represent both sides of the plate. A sheet of grafoil is introduced between the dies and they are pressed together forcing the grafoil into the desired shape. The application of pressure on the grafoil causes the graphite particles to orient themselves perpendicular to the pressing forces exposing the graphite to its least conductive orientation. The application of the pressures required in pressing has also created localized fissures in the material compromising the gas impermeability [17].

In both molding and pressing, dies for the plate and flow field channels are required. The manufacturing of these dies promotes long lead times, high production costs, and less flexibility in design change. They are particularly unsuitable for small batch production requirements that are present in current fuel cell research and development.

1.4 Thesis Objectives

The whole premise that the production cost of the fuel cell must be reduced in order that it be accepted as a viable energy conversion technology is the basis of this thesis. From the outset of this project the goal was to produce one component of the fuel cell stack, namely the fuel and oxidant delivery plates, at a greatly reduced cost while maintaining or enhancing its performance characteristics. Based on the cost comparisons discussed prior to this, the material and manufacture cost target of \$5 /plate was set as an initial goal. Other criteria that had to be met were: adequate conductivity, gas impermeability, and structural integrity.

The method of manufacturing that was chosen to pursue was screen printing. Granted screen printing is not commonly regarded as a manufacturing technique in the truest sense, but when applied to a problem such as the manufacturing of bi-polar plates, screen printing takes on a whole new role. The basic concept was to attack the problem from a different angle. Instead of sculpturing the material out, as is done with CNC machining, the required patterns and heights would be built up by a deposition process.

The project was initially staged to consist of two major phases. The first phase was to demonstrate the feasibility of using the screen printing technique to achieve the desired plate thickness and detail. The phase that followed was to concentrate on the second major hurdle anticipated which was the issue of conductivity.

1.5 Thesis Approach

The basis of the thesis was the introduction of an invention memo by Dr. Zuomin Dong, outlining the idea of using screen printing in a new approach to carry out the manufacturing of separator plates for a PEM fuel cell stack. The outset of the twelve month thesis witnessed a need to become affluent with two previously unknown fields, namely screen printing and fuel cell technology. Two simultaneous studies were begun in these areas.

The study of screen printing began with a literature search into screen printing, its history, previous and present applications, techniques both old and new, and apparatus used. Chapter 2 summarizes the findings of the investigation and highlights the important aspects involved in the screen printing process as it is known. Following the literary search and study, it was necessary to become familiar with not only the mechanics of the process but also the nuances of the art of screen printing. This was carried out with the help of the aforementioned Pat George and George Thiessen of the Department of Visual Arts at the University of Victoria. They taught and lent their years of experience to foster a small understanding of the art that enabled me to carry out the seemingly simple but realistically difficult task of producing quality screen prints.

The research into fuel cells began with a look at the basic fuel cell types, and principles of operation. Chapter 1 deals with these aspects and the motivations for pursuing the fuel cell as a viable transformer technology for the transportation industry. The more specific investigation of the technical requirements, material requirements, and current plate manufacturing techniques, aided by discussion with Ballard's Keith Prater, rounded out the study and is presented in Chapter 3.

With the preliminary investigations completed the thesis moved onto the next phase which consisted of printing separator plates. This phase involved the ongoing material selection for both the fuel cell environment and the screen printing operation, and the iterative approach of producing screen printed plates. Chapter 4 outlines the development of the screen printing process as it evolved into a viable technique, illustrating the screen printing principles that influenced the application.

Concurrent with screen printing technique development was the investigation into developing a suitable screen printing and fuel cell compatible ink. Chapter 4 lists the various materials tested and the results that were achieved with respect to environmental exposure and conductivity. Further investigations into two fields presented themselves as sources of understanding of conductivity behavior and were subsequently pursued. Microstructure investigation and Percolation Theory proved to be valuable tools in the pursuit of a highly conductive ink. Their study, presented in Chapter 4, identified new research paths with respect to the composition of inks.

The conclusions and thoughts towards future work for this thesis are presented in the final chapter, Chapter 5.

Chapter 2

2. Screen Printing-State of the Art

2.1 History of Screen Printing

Screen printing is essentially a stencil process. In its simplest form stenciling is carried out by forcing a pigment medium through an aperture or around a shape cut from stiff paper or a thin metal sheet. It is a process that dates back several thousand years. From the caves of early man in France to the walls, floors, pottery and fabrics of the ancient Egyptians, Japanese, Romans, and Chinese, stencilling has evolved into a highly intricate process that can be found in today's highest technology fields.

Stencilling, in its crudest form, is still used today for interior decoration and for marking containers and lettering, but as a method of reproduction it has its limitations. It is only suitable for the reproduction of relatively simple designs because the stability of a stencil relies upon the negative areas of the image to hold it together. The tie points greatly increase the delicacy of the stencil, and as such, limits the intricacy of the pattern that can be produced.

The Japanese are credited with overcoming this problem and evolving the stencilling process that laid the way for the development of screen printing as we now know it today. To solve the issue of tie points they cleverly cut two exact patterns of their design and then glued a human hair web across the face of one pattern to hold all the negative parts in position. The second pattern was then precisely laid over top of the web aligning the two stencils and glued into position to give a stable "sandwich" stencil. The

thinness of the hairs allowed the inks to pass through the stencil unobstructed and deliver the intricate pattern to the printing substrate. The use of human hair was eventually superseded by the use of silk strands, and it was at this level that the technology remained for several centuries.

It was not until the middle of the eighteenth century that stencil patterns were applied to silk meshes, and towards the end of that century the first silk screening equipment that is recognizable today, was used. In 1907 the first patent was filed for a screen printing process that made use of a silk mesh stretched over a frame and the paint being pressed through the screen using a squeegee. In 1915 the first photographic silk screen stencil was developed and it was from this point that the process became a common technique used in the printing and textile industry. By the 1930's automatic screen printing machines were introduced, paint was no longer used as the ink industry came on board and cloth manufacturers recognized the need to develop advanced materials to be stretched over the frames. Synthetic materials, nylon and polyester monofilament fabrics, were developed and replaced silk allowing a higher degree of accuracy. The result of all these advances was the introduction of "screen printing" as it is know today.

Advances in the industry have continued to this day, primarily in the printing process, ink and stencil areas. Automated printing machines have been developed that can screen print as many as 6000 imprints per hour (iph). The inks used have had to adapt to these fast printing speeds by rapidly drying, usually through accelerative forced drying, or more recently with the almost instantaneous effect of UV curing. Stencils now vary from the initial hand cut to the photomechanically made stencil.

Along with the technical developments of screen printing a diversity of application has also occurred. Screen printing is no longer strictly seen as a "printing" technique used

for posters and flyers, it has bridged the gap between art and high tech industry. Textile industries are perhaps the largest industry using screen printing extensively for printed fabrics. Plastics, ceramics and glass manufactures all use screen printing to a great extent. And perhaps the most advanced industry to make use of screen printing to date is the printed circuit board and touch sensitive switch manufacturer. In this application the electrical circuit is directly printed on the substrate using a highly conductive ink.

2.2 Equipment

A typical screen printing set-up consists of a frame over which the mesh is stretched, the mesh which supports the stencil, the stencil which is the design to be printed, a squeegee which is used to force the ink through the mesh, the ink which is the printing medium, the substrate which is to be printed on and the printing base which acts as a support structure for the whole assembly and allows for consistent registration. Figures 3.1 illustrates a typical screen printing arrangement.

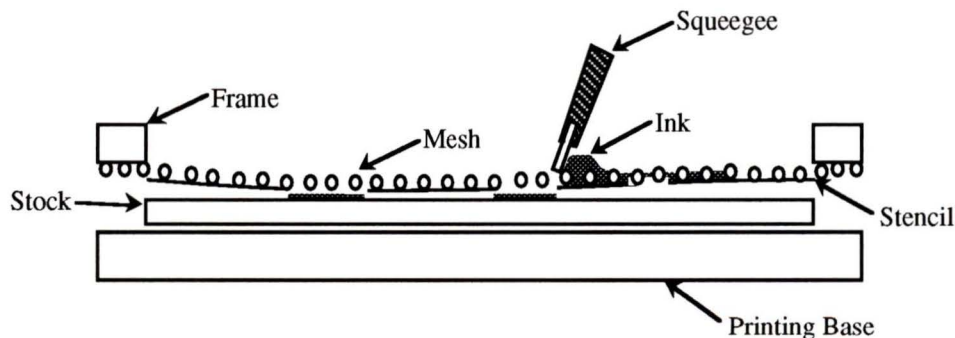


Figure 2.1: Typical Screen Printing Apparatus

2.2.1 Screen Mesh

In order to be used for screen printing the mesh material has to exhibit the following two requirements:

- It must provide an adequate support structure for the stencil.
- It must allow the free passage of the printing medium.

As stated above, silk was the original material used for screen printing. The silk yarn consists of a number of silk fibers spun together to form a multifilament thread. These threads are then woven into a mesh structure through which the ink material passes. The silk provided the support structure for the stencil but because of the uneven multifilament surface, clogging of the pores was a common occurrence causing a short print life. The uneven filaments also delivered inadequate sharpness of detail for modern applications. For these reasons, silk lost its place in the screen printing industry to synthetic materials, such as polyamide and polyester, which could provide fine monofilament fibres that are strong, chemically resistant, and have the ability to be manufactured with dimensional tolerances.

Synthetic screen meshes are classified by two methods. The first method is the mesh count. Mesh count denotes the number of single threads in the weave per linear centimeter or inch. The second method is the mesh grading. For this classification there are four categories: 'HD', 'T', 'M', and 'S'. The varying qualities relate to the relative fibre thickness that has been used to produce the mesh. HD stands for heavy duty, with the filament being rather thick, T stands for heavy quality, M for medium quality and S for light quality.

Screen fabrics are woven in a wide range of mesh counts. The lowest mesh counts are in the one to two threads per centimeter range while the higher counts are as high as 200. The lower counts are usually associated with the thicker filaments and the higher counts require the lighter fibre grades. The thickness of the fibre along with the mesh count determines the mesh openings. As the mesh count rises, the effective printing area of

the mesh is reduced, until a point is reached when the fabric no longer permits the printing medium to pass.

The mesh used will determine the print quality and particular characteristics such that various combinations need to be considered to achieve the ultimate goal. Two major factors to consider when selecting the mesh are:

- Ink film thickness.
- Stencil detail requirements.

The thickness of the ink film deposited is directly influenced by the thickness of the fibers used in making the mesh. Figure 3.2 illustrates how the thickness of an ink deposit varies with the thickness of the mesh filaments.

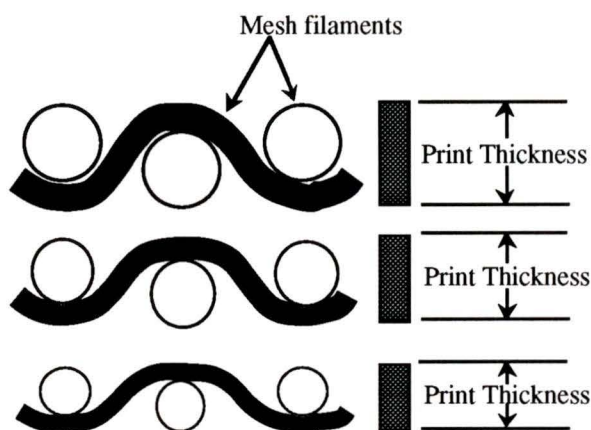


Figure 2.2: Screen Mesh Thickness vs. Print Thickness

The permeability of the screen mesh, and therefore its mesh count, will also determine the thickness of the ink deposit. A thick deposit, for example, is achieved with thick mesh filaments and a low mesh count. The low mesh count will also permit the transfer of any particles suspended in the ink onto the printed surface. Conversely, if a thin film is required then a thinner filament and higher mesh count would be appropriate.

The stencil detail is also affected by the mesh that is used. For applications requiring a high degree of accuracy with fine detail, a fine mesh is required to support the stencil. This consequently relates to a thinner ink deposit. When a thick ink deposit with fine detail is required, some compromises have to be made and the problem becomes a trial and error process to optimize the balance between the detail and ink film thickness.

2.2.2 Screen Mesh Materials

The use of different mesh materials also affects the printed result. Nylon (or polyamide) is a common material used for monofilament mesh construction. It is durable and exhibits elastic characteristics which make it suitable for printing on uneven surfaces. Polyester mesh is also a common mesh material, with very different properties. Polyester mesh fibers are very regular dimensionally, which lends their application to precision and fine detailed screen printing. Polyester also has a greater resistance to extension and does not absorb moisture as does the nylon. These properties translate into a much more dimensionally stable material that is used in applications requiring dimensional stability in the screen, such as the need to have a high degree of registration repeatability. Polyesters' durability also make it a suitable material when a number of print runs are required.

The use of coloured mesh is becoming more common with both the polyamide and polyester materials. The meshes are died either red, yellow or orange to prevent the effects of light scatter which can occur when exposing a direct screen to ultraviolet light, in direct stencil making. If white mesh is used for a direct stencil, the surface of the mesh will reflect a certain amount of the actinic UV light within the mesh structure. The actinic light is the light which will produce a chemical reaction in the photosensitive stencil material. This reflection can cause areas of the stencil to be exposed that otherwise would not be and

thus causes what is known as image undercutting. Image undercutting will reduce the overall dimension of image reproduced on the stencil. For finely detailed print production this dimensional instability can be a significant problem. Using the coloured mesh helps reduce, and may even eliminate, the undercutting effect as it absorbs the actinic light and reflects the other non-destructive wave lengths. Figure 3.3 illustrates the actinic light absorption problem.

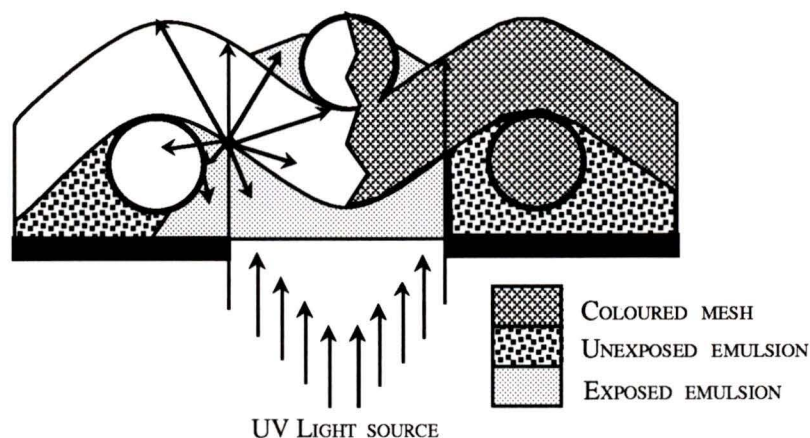


Figure 2.3: The Effects of Light Scatter. Coloured Screen Mesh Absorbs Actinic UV Radiation

For high precision printing, where dimensional stability is the most critical factor there exists two screen material options. Metallized polyester and the more expensive stainless steel mesh are the choice for high tolerance applications such as the printed circuit board industry. Metallized polyester is made by coating the polyester mesh with nickel. The result is a much stiffer mesh and an enhanced ink passage due to the filling of small fissures at the thread overlap points. Stainless steel mesh goes even one step further. Its unmatched dimensional stability meets the strictest demands of the printed circuit industry. Stainless mesh also has the highest permeability when compared with other meshes of the same mesh count, due to the small diameter of the wire used to weave the mesh as compared to the synthetic fibers. The increased durability of the metallized and stainless steel meshes allows them to be used for a far greater number of printing runs when

compared with the synthetic materials. Unlike the synthetic fibers, the metallic meshes do not absorb moisture and are therefore unaffected by changes in humidity. They are also free from temperature change effects.

The nickel coating and stainless steel also make these meshes electrically conductive. This allows for the shedding of static electricity which can build up as a result of the squeegee passing over the screen. The build up of static charge can cause serious problems when using automated printing machinery. The metals also allow the screens to conduct electricity for use in thermoplastic printing applications. In this operation a thermoplastic powdered ink is heated during the printing process. The special ink melts and passes through the mesh onto the substrate where it fuses immediately into a solid film.

These outstanding benefits do not come without a few drawbacks. The most obvious is the cost of the materials. The metallized and stainless meshes can cost up to three times that of the synthetic fibers. The added cost may, however, be made up in the increased durability of the screens and the precision gained by their use. The metallic meshes are also susceptible to mechanical damage and as such must be treated very carefully when handled.

2.2.3 Frame

There are a variety of frames that can be used in a screen printing operation. Their construction can be of wood, steel, aluminium or plastic. The essential requirement for the frame is its rigidity. Having the mesh stretched and tensioned over the frame must not allow any distortion in the frame. Even the smallest amount of distortion will affect the quality of the print. The selection of the frame material must consider the size of the frame to be used, and the tension that is to be applied over the mesh. The warping of a frame

under tension will cause problems in off contact adjustment and print release, both critical for good print definition. If the frame bends it will also affect the tension distribution throughout the mesh and cause a loss of dimensional stability over the mesh. The weight of the frame must also be considered when it must be handled frequently. With these points in mind the selection of the frame material can be made appropriately.

The tensioning of the mesh over the frame is considered to be one of the critical steps in the printing operation. There are several methods that can be used for tensioning a screen, but the most commonly used is the pneumatic tensioner. A series of pneumatic clamps stretch the mesh over the frame and the tension applied is monitored with pressure gauges on each clamp. Once the appropriate tension is set the mesh is fastened to the frame and the clamps are removed. The tension is then checked once again to ensure a proper distribution over the frame.

2.2.4 Stencils

There are several methods by which a stencil can be made, but they must all perform the same function: to block the non-printing areas of the screen and to provide clear, well defined open areas to form the printed image. There are two distinct categories of stencils based on their methods of preparation:

- Handmade stencils.
- Photomechanically made stencils.

Among the category of handmade stencils there are hand painted stencils and knife-cut stencils. Hand painted stencils are produced by working directly on the screen with block-out filler and/or a wax resist. Knife-cut stencils are made by cutting around the stencil image with a sharp knife, removing the open areas to be printed and then adhering the stencil to the screen.

Photomechanically produced stencils, the more commonly used method today, consists of: indirect photostencils, direct emulsion photostencils, direct/indirect photostencils, and capillary direct film photostencils. Indirect photostencils are made by contacting an opaque positive image to a light sensitive stencil film which is transferred to the screen mesh after processing. Direct emulsion photostencils are made by coating the screen with a light sensitive liquid emulsion which is exposed in direct contact with an opaque positive image, the stencil being formed directly in the screen mesh. Direct/indirect photostencils are a combination of the above methods in that the stencil is made by bonding a film coating to the underside of the screen with a light sensitive liquid emulsion, and exposing it in direct contact with an opaque positive image. Capillary direct film photostencils are made by mounting a light sensitive film coating onto the screen and exposing it in direct contact with an opaque positive image.

The various types of stencil production have their pros and cons and their use is dictated by the particular application. In the high tech printed circuit industry the preferred stencil type is the direct/indirect photostencil. The properties of the direct/indirect photostencils that promote its use in this industry are:

- the stencil is made from polymer coating which provides a guaranteed stencil thickness,
- the stencil has a very smooth underside thus eliminating the capillarity which can occur at the stencil/substrate interface eliminating microscopic ragged edges
- the stencil has excellent durability allowing for long printing runs, and,
- the stencil has excellent resistance to aggressive solvents and to abrasive inks, such as those containing small particles.

The selection of the appropriate stencil type is just the beginning of the stencil production process. Each type of stencil material has distinctive preparatory steps, the details of which are far too extensive to list here. Suffice it to note that there are several key issues regarding stencil production that must be considered. Preparation of the screen mesh comes first, followed by mounting of the screen, calculating the proper exposure, exposing the screen, and then washing the exposed material away. Each of these steps must be completed to a high level of competence in order for the end result, the print, to be of satisfactory quality. In some instances, such as printed circuit work, a number of these steps are carried out mechanically. The automation of these steps allows for careful monitoring of all the variables and a high level of repeatability.

2.2.5 Squeegee

The squeegee performs a very important function in screen printing. It is used to force the ink through the screen mesh and stencil onto the printing stock below. The ink is pushed through the screen and stencil by the forces created in it through the action of the squeegee during the printing stroke. A pressure wave is set up by pulling the squeegee across the surface of the screen and the resistance of the ink, resulting in a flow of the ink in the direction of least resistance through the screen. Figure 3.4 illustrates this principle [10].

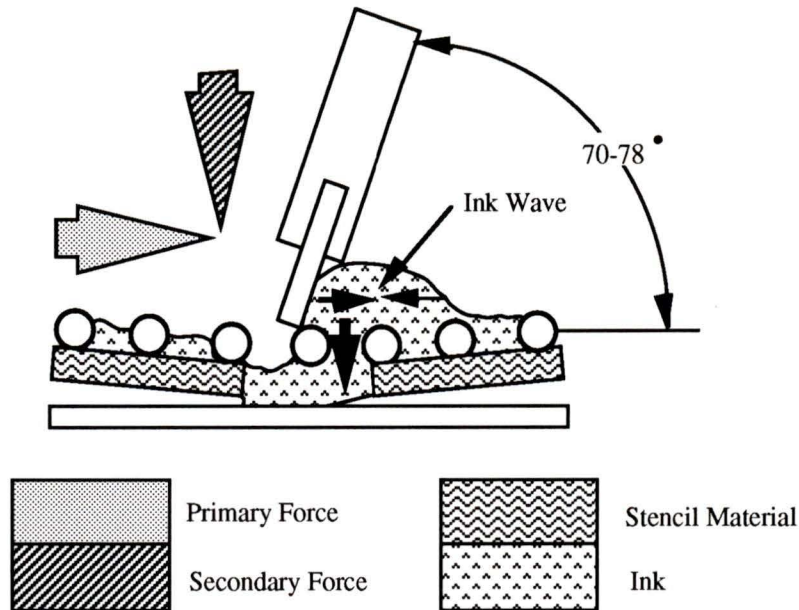


Figure 2.4: Ink Flow as a Function of Squeegee Angle

There are several factors that influence the way the ink passes through the screen. The angle created between the stencil and the squeegee determines the magnitude of the pressure wave created as the squeegee is dragged across the screen surface. The maximum pressure angle is created when the squeegee is pulled at an angle of 70-78° [12]. Outside of these angles the strength of the pressure wave falls, potentially resulting in a failed print. The shape of the squeegee tip also influences the way in which the ink passes through the screen. Figure 3.5 illustrates the various squeegee blades currently used.

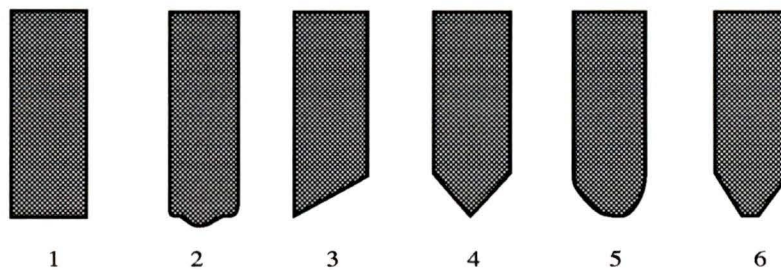


Figure 2.5: Squeegee Blade Types

The square-edged blade provides a thin ink deposit on flat surfaces and is typically used for graphics printing. The small radius round-edge blade is used for both graphic and

industrial applications, again for flat surfaces but with thicker ink deposits. The single beveled-edge is used for flat printing on to non-absorbent surfaces such as glass or metal. The doubled beveled-edge is used for printing onto curved surfaces. The large radius round-edge blade is used for forcing ink into an absorbent material such as textiles. The double-sided flat-edged bevel blade profile is used in ceramic printing. The choice of squeegee blade depends on the application, but the testing of different profiles should be carried out to ensure the desired printed effect.

2.3 Inks

The number of inks available to the screen printer today is astounding. For almost every conceivable type of screen printing there are several options for inks. The various types of inks are typically classed into one of the following categories: long oil alkyds inks, synthetic thin film inks, ultra thin film inks, vinyl inks, two pack catalytic inks, and UV drying ink. The selection of the type of ink to use is up to the printer and usually depends upon the application, screen printing technique, printed substrate, drying technique, and whether the printing is a high volume process or not. General properties to consider when choosing a screen printing ink are: printability and rheology, adhesion, and drying [12].

The printability of an ink refers to its ability to pass freely through the screen mesh and not obstruct any openings. The ink must have specific flow and deformation properties which allow it to pass through the screen freely and then form a solid film on the surface of the substrate. If an ink is too thick, it will not flow properly once it has passed through the screen, leaving a checkerboard pattern caused by the mesh. If the ink is too thin it will flow too freely through the mesh and will not hold the desired shape, and may result in “bleeding”, which is the capillary action of the ink between the stencil and substrate.

Adhesion of the ink to the substrate is perhaps the largest source of variety among ink types. Different materials require different bonding agents, and some materials like plastics need to bond both physically and chemically to the substrate.

The choice of ink drying technique will also contribute to the ink type used. There are four commonly used ink drying techniques: oxidation, solvent evaporation, infrared curing, and ultra-violet curing.

Oxidation is the oldest of the drying techniques used and relies on the oxidation of the oil used as the vehicle [11]. A typical application using oxidation as the drying vehicle will require 6-8 hours to dry at room temperature. For this reason it is rarely used for high volume production.

The majority of screen printing inks are solvent based and dry by evaporation of the solvents. The solvents used vary with the materials onto which they are printed. Solvent mixtures are added to inks in complex mixtures such that the particular solvents' evaporation rate is tailored to the specific application. If a solvents' evaporation rate is too high it will not only dry on the material quickly, it will also dry on the screen mesh rendering it unuseable. On the other hand, if the solvent dries too slowly it will take excessive time to dry slowing down the printing process. Solvents are also used to dissolve resins so that they may be mixed with other ingredients, and in some cases are used to reduce the viscosity of an ink mixture.

An increasingly popular type of ink being used in the printed circuit and textile industries is the infra-red (IR) cured ink. In most cases the printing medium is based upon a resin which will polymerize when exposed to intense IR radiation. The cross linking of

the polymer produces a solid film of great permanence and with excellent chemical and solvent resistant properties. Two types of IR radiation are used and the selection of the type will depend on the substrate being used. For temperature sensitive substrates a medium or long wave IR emitter is used. These emitters operate at 800-950°C as opposed to the short wave IR emitters that operate at about 2200°C. Both types of emitters will drastically reduce typical drying times from hours to seconds.

The newest ink drying method to be developed is the ultra-violet (UV) curing technique. This technique is based upon the principle of photopolymerization. The inks contain photosensitive resins which react chemically when exposed to intense UV radiation. The process is a three step curing process: photoinitiation, polymer propagation, and polymer termination. The photoinitiation process begins with the creation of reactive free radical intermediates, formed by the action of UV radiation. The polymer propagation takes the free radical intermediates and reacts them with available monomers to form a long chain. When all the monomers have reacted polymer termination has occurred resulting in a stable long chain polymer.

This whole process occurs in a fraction of a second solving the problem of screen stability and drying time for the mass production operation. With the UV ink it is possible to print the finest detail, since the mesh will not become blocked by dried ink. One other key feature of the UV ink is that since there is no evaporation of solvent, the ink deposit remains 100 percent of its original print thickness. This characteristic requires careful consideration of the screen mesh and the stencil thickness to control the deposit thickness. The end result, however, is a highly detailed and repeatable deposit. Industries like printed circuit manufacturers are increasingly making use of the newer ink technologies to deliver high quality products.

2.4 Printing Machinery and Techniques

Screen printing has evolved for over a century into a highly mechanized and automated production process. The screen printing machinery used today consists of components that are fundamental to the original hand-bench printing equipment. A typical hand-bench setup will consist of the following components:

- A flat printing base with some allowance for holding the printed substrate in position. This typically takes the form of a vacuum suction table.
- A frame clamping system.
- A hinge assembly which permits the raising and lowering of the clamped frame.
- A registration device.
- Off contact adjustments.

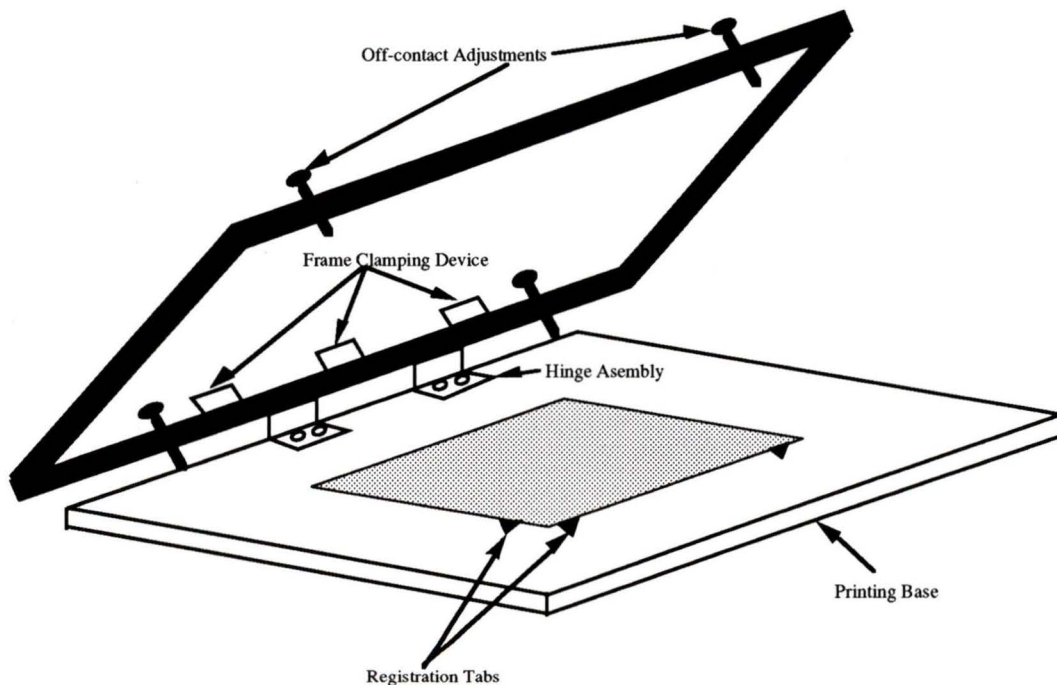


Figure 2.6: Typical Hand-bench Printing Set-up

The printing base is typically made of a material that is rigid, flat, and allows for the inclusion of fine holes to be used as a vacuum hold-down device. The frame clamping device must be very rigid and capable of holding the frame and screen assembly with no

deformation under stress. The frame clamps must also allow for quick and easy change of the frames.

Registration is the alignment of the print stock in relation to the stencil. For multiple prints where the stencil must be changed or cleaned between prints, registration is vital. There are several methods to achieve good registration. One method is to place registration tabs on the printing base which allows the removal and replacement of the printing stock. The use of adjustment screws on a floating printing bed or on the screen frame holder also allow for accurate registration. Without an adequate registration system precision printing is impossible.

The final key component of the bench printing apparatus is the off-contact adjustments. Off-contact distance refers to the distance between the underside of the screen and the printing surface. Its adjustment is critical to print quality by influencing the rate at which the print is released from the screen. In most instances printing is carried out with the screen out of contact with the printing surface. The reason for this is to allow the print to release rapidly from the screen, thus preventing the tendency for the ink to flow laterally between the underside of the stencil and the printing surface. The amount of off-contact distance required is a function of the following variables:

- print area
- tension of the screen
- ink viscosity

The print area refers to the physical area of the print. The larger the print area the greater the off-contact distance that is required. This is due to the large area of ink contact between the screen and the printing surface which in turn results in a higher resistance to separation.

The tension of the screen also determines the amount of off-contact distance that is required. The screen's tension determines the speed at which it regains its original shape after having the squeegee pass over it. The tighter the screen the faster the release and the less off-contact distance required. It is also interesting to note here that in the case of an under tensioned screen, the off-contact distance needs to be increased to compensate for the slow release rate, which in turn increases the deformation of the screen and reduces the dimensional stability of the print. Thus for precision work the screen tension should be adequate to minimize the off-contact distance required.

The viscosity of the ink is also a contributing factor when determining the off-contact distance. The more viscous the ink the greater the resistance to the shearing forces present as the screen lifts from the printing surface. The off-contact distance therefore needs to be increased to elevate the lifting forces such that the release rate is adequate to give a good print quality. The alternative is to thin the ink with the addition of an appropriate thinner. Figure 3.7 illustrates the principle of off-contact adjustment [12].

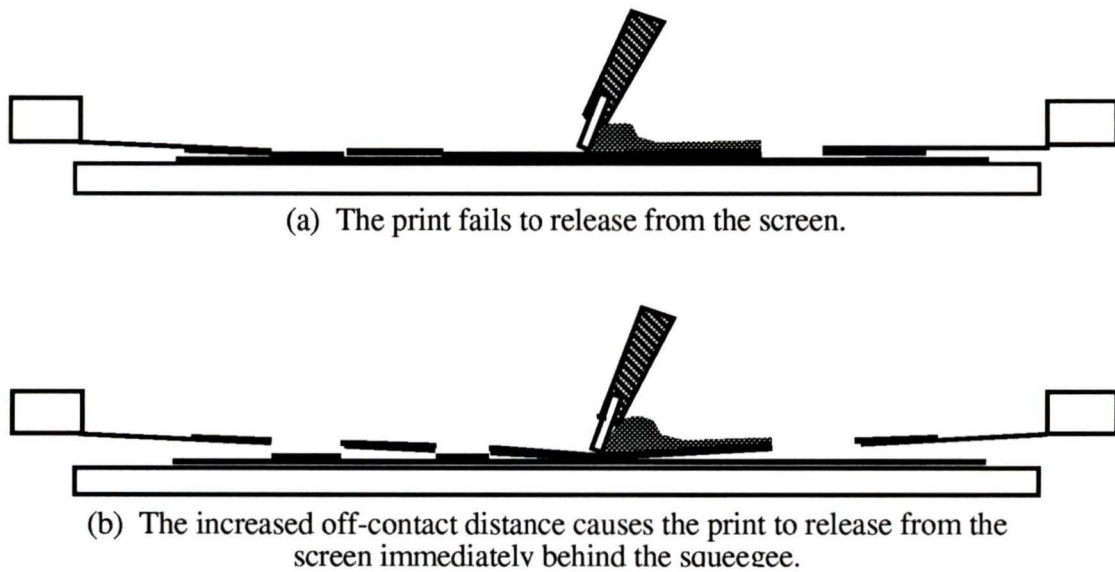


Figure 2.7: Principle of Off-Contact Adjustment

In the mechanized screen printing machine, the features mentioned above are all taken care of automatically, with fine tuning done by the operator. There are several different types of automated screen printing machines and they generally have specific applications. Some of the more common types of machines in use today include: the flat-bed hinged frame, flat-bed vertical lift, the cylinder-bed press, container printing machine, and the rotary screen printing machine. Schematics of these printing machines are illustrated below [12].

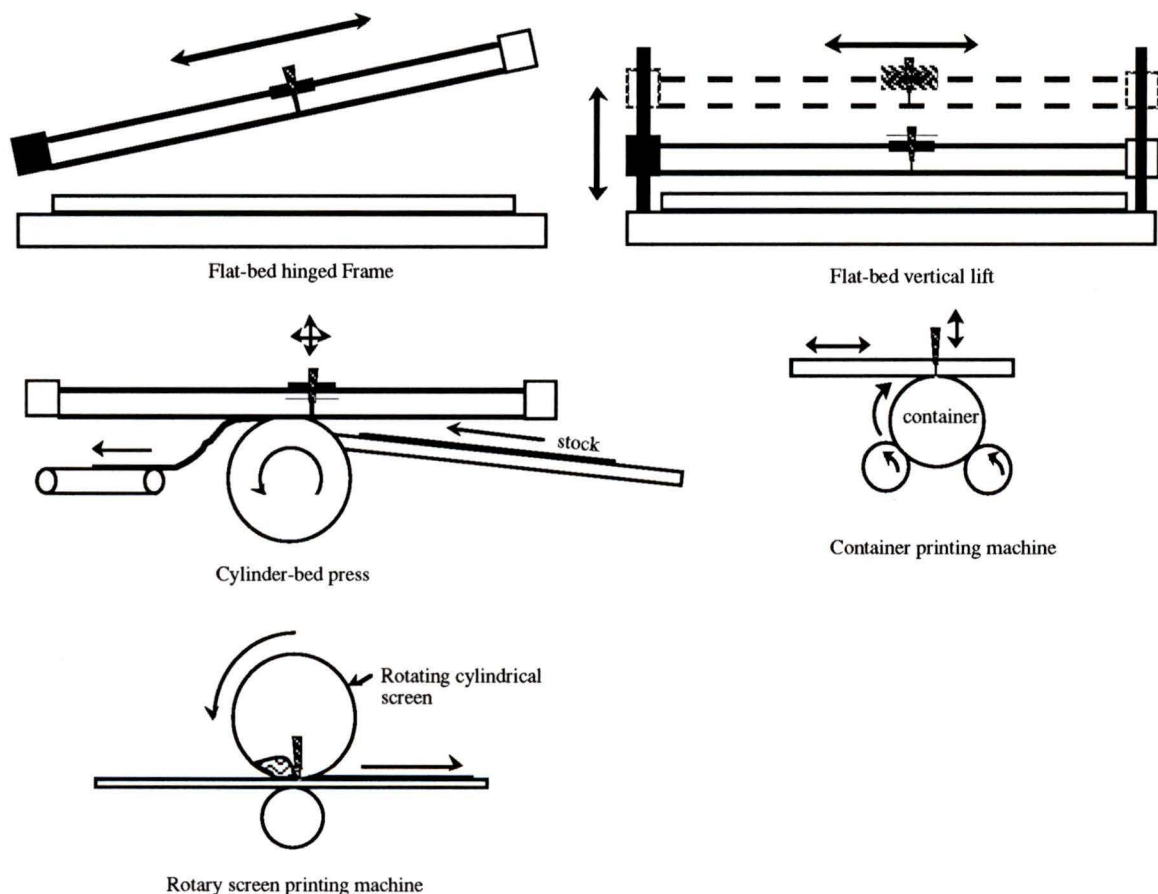


Figure 2.8: Common Printing Machine Arrangements

The flat-bed hinged and vertical lift printing machines are little more than automated hand-bench printing devices. The automation consists of the lifting of the screen between

prints, the automatic feed of the printing stock, and the automatic operation of the squeegee. The adjustments available include pull speed, squeegee angle and pressure, and stock feeding speed. The vertical lift apparatus has the advantage that it only needs to lift the frame assembly a few millimeters to change the print stock, thus increasing its possible number of impressions per hour (iph - the commonly used term for measuring the printing speed). Fully automated versions of the hinged and vertical lift flat-bed printing machines are capable of printing up to 2000 iph and 2500 iph respectively.

The cylinder-bed printing machines typically change the way in which the printing stock is fed through the system. Instead of the stock remaining stationary and the squeegee moving across its surface, the stock is picked up by a vacuum cylinder and rotated. The squeegee remains fixed and the stencil is reciprocated between the squeegee and the rotating cylinder. These machines are limited to the use of flexible stock and have printing speeds of up to 6000 iph.

The container printing machine is very similar to the cylinder-bed printer except that the vacuum cylinder is replaced by the container that is to be printed on and the container is held in place by a series of rollers. The size and shape of the containers can vary and the speed of the operation depends on the complexity of the shape.

Rotary screen printing machines are a combination of the other printing machine technologies. The cylinder in this case performs the roll of the screen. The squeegee is held in place within the cylinder and the ink is passed through the squeegee to the screen surface. The printing stock passes on a conveyor system beneath the cylinder. This set-up allows for continual pattern repetition that is seamless and as such is the choice of the textile industry for applications like curtains, fabrics and wall coverings.

There are several other forms of printing machines available but they are usually customized for particular applications. The previously mentioned machines illustrate the varied applications that are possible with screen printing and the ability for the process to be used in a batch or mass production environment. The relative cost of these machines varies with the application. Rotary screen printing machines for example have a relatively high capital cost and require specialized screen preparation and development apparatus which also raises the cost. Flat-bed hinged and vertical lift machines however, are relatively cheap to construct and can still provide a high volume operation.

Chapter 3

3. Screen Printing Applied to Manufacturing of Flow Field Plates

3.1 Motivation for Using Screen Printing

The cost of production of a fuel cell flow field plate is an inhibitor to the acceptance of the fuel cell driven vehicle as a viable alternative to the internal combustion engine. For this reason, alternative manufacturing processes are being investigated by the major fuel cell manufactures. The feasibility of using screen printing as a plate manufacturing technique was the focus of this thesis and was proposed in an NGFT invention memo [27]. What makes screen printing an exciting proposition is its ability to overcome the majority of the problems associated with the present state of the art for the manufacturing of the flow field plates. The primary motivators for using screen printing are: lower labour and material costs, simple automation to permit the batch or even mass production, low capital costs associated with batch and mass production, and the ability to rapid prototype [27].

When compared with the current practice of CNC machining of the flow field plates, the issue of labour costs appears to be a rather significant factor. In the machining process there must be a highly trained CNC machine operator present at all times. His/her function is to oversee the machining process, control the cutting speeds, monitor the tool bits for wear, and change the bits when required. The entire evolution takes an average of two hours per plate [17]. When the machining is complete the plate must then be inspected for any flaws that may have appeared during the process but were not picked up by the operator. Such flaws become crucial when you consider the outcome of them being undetected. Possibilities include the permeability of gases across the plate and breaks in the

electrical continuity. Both of which could introduce drastic performance reducing and safety problems.

In the proposed screen printing process the labour costs could be cut significantly. The operator of the screen printing machinery, although skilled is much less so than the CNC mill operator. The demands on the printer are less stringent and as such allow for a lower basic labour rate. The time required to produce a plate is also anticipated to be much less than that of the CNC mill. A plate could be produced in under ten minutes being a reasonably conservative estimate. Thus an overall significant savings on the labour costs are expected through the use of screen printing.

In terms of material costs, screen printing offers several advantages. In the CNC operation material is cut out of an existing block thus wasting a certain percentage of the material. Screen printing on the other hand, builds up the required dimension and as such has no inherent material wastage. When considering the preprocessing costs of the graphite plates used in the milling operation, even a 10 percent reduction in material costs through wastage removal adds up to a significant total. The material costs themselves are also significantly less for the screen printing process. Instead of requiring a preprocessed, gas impermeable, and flat graphite plate as the base of the product, the screen printing material requirements are based on graphite powder and a liquid that is used as the vehicle and binder. Obviously the cost of the graphite powder is considerably less than the base price of the graphite plate, and the cost of the liquid additive is considerably less than the remaining pre and post processing costs.

The acceptance of the fuel cell as a viable conversion technology in the transportation market will initially demand a viable batch production plate manufacturing method. This may be achieved by the present technology, but at a very high capital cost.

Considering that for each plate, one CNC milling machine must be dedicated for a period of up to two hours the required number of milling machines, and subsequently capital and labour costs, for even small batch production is considerable. Screen printing machinery on the other hand is inherently cheap when compared to a CNC milling machine. For example, a fully automated vertical lift flat-bed screen printing machine capable of 2500 paper iph would cost in the order of \$5,000-\$10,000 [11]. A milling machine could easily cost \$100,000. The capability of the screen printing machine to out-produce the milling machine broadens the financial gap between the two technologies. Screen printing could be capable of filling a batch production requirement with only a small amount of technical development.

When considering a mass production process, the option of using a milling operation is no longer viable. The number of machines and operators necessary preclude this technology as an option. Screen printing, however, has the potential of producing a printed plate in as little as a fraction of a second (using UV technology). This potential not only surpasses current technology production capabilities, it leaves the option to mass produce open for screen printing with only minimal technical development.

An additional attractor to the use of screen printing as a flow field plate production technique is its inherent ability to rapid prototype. With an established printing environment the time required from flow field design conception to actual prototype testing can be measured in hours as opposed to days or even weeks in conventional manufacturing processes. Computer assisted designs can be printed onto acetates that are used to develop the new patterns onto the printing screens. These screens are then simply loaded onto the printing apparatus, trial prints carried out and adjustments made. The end result is a functioning prototype ready to be tested in the fuel cell stack in a matter of hours. There is no need to develop expensive toolings, produce expensive molds or carry out extensive

machinery set-up. This is an attractive option not only for the finance department, it is also exciting for the designer who can quickly test new ideas.

3.2 Technical Requirements and Objectives

In order for the use of screen printing to be accepted as a viable plate manufacturing technique for PEM fuel cell flow field plates it must satisfy several criteria. Among these critical requirements are: deposit thickness, acceptable conductivity, surface finish, chemical stability, structural integrity, and substrate bonding.

The deposit thickness refers to the thickness of the built-up channels as measured from the bottom of the channel to the upper surface. This is a critical dimension for the flow field designer as the flow of gases and in some cases liquids depends on this dimension coupled with the channel width. As discussed with Ballard it was decided that a minimum channel depth of 0.7 mm be chosen as the target that screen printing had to achieve [17]. At the same time the resultant print has to be clean and follow the detail as prescribed by the original pattern. Deviation from the outlined dimensions could result in a degradation of the cell performance and even cell failure. The requirement of printed width was never set leaving the print trial to determine the range of possibility.

The next and perhaps the most challenging of the criteria for the screen printed plate is the conductivity. For this requirement it was decided to use the present graphite plates as a benchmark. The target set at the outset of the project was to come within one order of magnitude in relation to the plates bulk resistivity of 10^{-3} Ohm \cdot cm. Good conductivity is also measured in terms of maximum plate losses. A typical Ballard MK V stack exhibits 50 mV/stack loss [17]. This target, although difficult to measure without a full stack, was also considered. The surface resistance of the plate should be in the order of 0.01 Ohms \cdot cm².

The surface resistance includes contact resistance, resistance of any oxide layer and the resistance of any protective coating.

In terms of chemical stability the plates must be capable of withstanding the harsh fuel cell environment without breaking down. Current specifications for plate durability require the plate's structure to remain stable and in tact for a minimum of 5000 hours of use. This translates into over 208 days and as such this test was unable to be carried out. Exposure of the plate materials to a humid fuel cell-like environment would substitute for the above test. The plate must also exhibit an impermeability to the passage of hydrogen from one side to the other. This requirement is in place for obvious safety reasons. After discussion with Ballard it was decided that an acceptable limit for an 8" x 8" plate would be <3 cc/min for a 0.15" thick plate with 30 psig air on one side at room temperature. . The plate must also not contaminate the membrane with positive ions or leach ions into the de-ionized cooling water which would cause electrical shorts.

The printed plate must maintain its structural integrity under the compressive loads of the fuel cell stack, approximately 100 psi [17]. These loads are required to maintain the stack form and provide sealing forces around the perimeters of the plates. Along the same parameters the ink and substrate must form an adequate bond such that there is no separation or delamination.

The surface finish of the printed plate is also of concern in terms of sealability and contact with the MEA. Contact with the MEA in only certain sections of the active area will cause localized hot spots. These in turn may cause hydration problems with the membrane and in the areas of inadequate contact pressure the contact resistance will increase reducing the overall performance of the cell. The close tolerances required of the machined plates on the other hand may not be necessary due to the design characteristics of the TERS stack.

3.3 Material Selection

When considering screen printing as a manufacturing process for bi-polar plates it was necessary to break down the material requirements and assess each component for compatibility in terms of screen printing and the fuel cell. The material selection was based on several factors. The cost was one of the leading influences on material selection as this project's goal was to reduce the overall manufacturing cost. This criteria eliminated the use of any exotic materials like platinum or gold as fillers. The materials ability to meet or exceed the technical requirements listed above was also a selection criteria. The various stages of the project that required careful consideration with respect to materials were: ink base material, printing substrate and solids loading materials.

3.3.1 Ink Base

The ink base material had to possess certain characteristics to warrant its selection. Primarily the ink base had to be screen printable. The viscosity of the ink base had to be such that it would accept the addition of a conductive filler (although if a conductive ink base were available this would not have been a requirement) and remain printable. The viscosity of the ink could be altered by the use of appropriate thinners but this could potentially result in undesirable effects like cracking upon drying. The ink base also had to demonstrate resilient qualities as it was most likely to be printed on a very thin and flexible substrate. The cracking of the print would result in the loss of conductive properties and potentially gas leaks.

The ink base is also required to withstand the environment of the PEM fuel cell. A PEM fuel cell environment is typically acidic with an operating temperature of 70°C-

100°C and 100 percent relative humidity. While exposed to these conditions the ink base must not breakdown chemically or mechanically. Chemical degradation may result in the damaging or clogging of the MEA. The ink base must be capable of maintaining its printed shape under the clamping forces used to hold the stack together and the loads induced by thermal expansion.

Ink base materials that were initially considered included: graphite pastes, standard screen printing inks (a large variety of which were considered), inks used for printing of circuit boards, conductive epoxies, conductive silicones, and low viscosity epoxies and resins. The screen printing inks fall into two basic categories, oil based and water based. Under these two headings there are a multitude of different ink types. Advice from the Art Department led to the selection of a water based standard poster ink. Several varieties were tried and the ink that produced the best printing results was TW Graphics' WB5101.

3.3.2 Printing Substrate

The selection of the printed substrate was conducted with the following properties in mind: conductivity, thinness and flexibility, non-metallic, off gassing potential and gas impermeability. Ideally the substrate was as conductive as possible. The thinner the plate the better as a thin plate helps to reduce the overall dimension and weight of the stack while at the same time improving the conductive properties. Metallic materials were not considered for a number of reasons. The first reason was that the jury is still out on the use of many metals in the PEM fuel cell environment. It is thought that metallic ions migrate to the MEA and clog or damage the material, shortening its useful life. Special coatings are being investigated that would prevent this from occurring, but it was decided not to rely on their success. The second reason for not using metals is the formation of oxide layers on the metal surface which would hinder the passage of electrons and compromise the

adherence of the ink base. This situation would require careful attention to overcome and once again the focus of the project was to prove the feasibility of the printing. In the event that the use of metals is proved feasible they should be included in the list of possible substrate materials.

Gas permeability of the printed substrate was also an important criteria considered. The gas permeability limits that were adopted came from Ballard. For a typical 8" x 8" Ballard plate, 0.150" thick with 30 psig air on one side, at room temperature the permeability limit is 3 cc/min [17].

Materials that were considered for the printing substrate included conductive plastics, and grafoil. Investigation into the plastics revealed that they tend to outgas under fuel cell operating conditions. The gases produced contaminate the MEA and cause performance degradation eliminating the possibility of using plastics. The second option, grafoil, was recommended as a likely candidate in the NGFT invention memo [27]. Grafoil is a trade name of Union Carbide. Similar graphite foils, like Calgraph, are also available from other suppliers like Polycarbon. For the purpose of the investigation both graphite foils provided similar characteristics.

Grafoil, a flexible graphite sheet, is a 100 percent pure graphite material. It is manufactured from exfoliated (expanded), highly crystalline graphite flakes, which are pressed into foil through an extensive calendering process. It is through this operation that individual expanded graphite flake particles are mechanically locked together without the use of fillers or binders. After calendering the foils are further processed into a variety of forms and grades. Some of the published material characteristics include: resistant to high temperatures, no aging or embrittling, excellent thermal stability, low thermal expansion,

chemically inert, highly flexible, high purity, high thermal conductivity, low permeability, low electrical resistivity, and chemically resistant.

The electrical resistivity typical of a grafoil sheet is 0.001 Ohm ·cm parallel to the surface and 0.0625 Ohm ·cm normal to the surface [21]. The air permeability of the foil was rated at <0.00002 cm²/sec [21]. Both of these properties were within the limits set out initially.

Grafoil is available in a variety of grades and thicknesses. The grades selected were the high purity nuclear grades. They were chosen over other grades because of their purity and the subsequent lack of off gassing that may occur with the lower grade foils.

3.3.3 Conductive Filler Material

The selection of a conductive filler material was begun with a look at other conductive materials that have a filler material added to promote conductivity. Printed circuit board inks typically contain silver, copper, or gold particles. Both gold and copper were eliminated from this list; gold because of the expense and copper because of its tendency to breakdown and release Cu²⁺ ions which would damage the membrane. Silver was considered because it has a slight catalytic effect. Stainless steel was also considered as it is the one metal considered slightly fuel cell friendly. Other conductive materials like silicones or epoxies use these same metallic particles and also graphite powders. Artificial graphite is highly conductive and considerably cheaper than metallic particles.

The artificial graphite powder arrived in a bulk state. A sifting machine was used to separate the graphite into three useable grades: 1μ-53μ, 53μ-75μ, and 75μ-150μ. The

upper size was limited by the screen mesh and the inks' printability. The use of particles too large resulted in scratching of the stencils, damaging of the screen mesh, and clogging of the passages.

Chapter 4

4. Printing Techniques and Ink Development

4.1 The Evolution of Thick Deposit Printing Technique

When considering using screen printing as a possible fuel cell flow field plate manufacturing technique, the initial and perhaps most significant hurdle to overcome was how the channel height was going to be achieved. The target of 700 microns was considerably greater than what is produced with today's screen printing techniques. A typical screen printed layer is in the order of 10-30 microns thick. Advancements in printing technology have reduced the thicknesses rather than increased them. For this reason the process used would be bucking the tide of progress and current industry procedures would be of little use.

Several approaches to the problem of achieving the required thickness were considered. The approaches can be broken down into three philosophies: use a thin stencil and build up the thickness by multiple layering, use a thick stencil and achieve the print thickness in a single print, or use a medium thickness stencil and do a combination of the multiple print and thick stencil approaches.

Several issues must be considered with each stage of development. Ink composition, mesh size and stencil manufacture must all carefully be monitored and evaluated. The ink composition that was chosen as the standard basis consisted of 40 weight percent graphite and 60 weight percent WB 5101. This mixture provided a

printable ink with good pull characteristics. The screens that were used varied from 90 to 140 mesh.

The first stencils used for the multiple layering technique were produced by coating a screen mesh with a photosensitive emulsion four times and exposing this to a hand-cut positive of the plate design. The thickness of the stencil was measured to be approximately 20 microns. Printing was carried out using a hinged flat-bed printing apparatus onto a grafoil substrate. The registration system used was a three pin system, having punched three holes in the grafoil and placing metal tabs onto the printing base. Initial prints on the 140 mesh screens were encouraging, the ink deposition thickness was approximately 17 microns per print. This translates into 41 prints to build up the 700 micron channels. The registration of the prints was quite good initially, but began to breakdown once the 28th layer was applied. The reasons for this can only be speculated at but it was believed that the seating of the stencil onto the printed surface became problematic and as a result the stencil would shift with the pressure of the squeegee passing over it. The maximum depth of channel that was achieved using this method was 0.2 mm. With improved registration methods and automation it is felt that this process would eventually be capable of achieving the full height, but to reach this goal would require further investigation into the progressive increase of off-contact adjustment and squeegee pressure.

The different mesh sizes that were tried had varied results. The 90 mesh screen was more difficult to pull and quite often the larger mesh would have overlap problems. This was caused by the stencil breaking down due to the lack of bonding surfaces on the larger mesh and the deformation of the screen. For this reason the 140 mesh screens performed the best and gave the most detailed and consistent results.

The outcome of the initial tests were very encouraging. The adherence of the printing ink combined with the graphite powder was good, exhibiting a strong bond to the surface and good flexibility. Shrinkage occurred in the vertical direction of up to 50 percent with very little in the horizontal direction. Dimensional stability in the horizontal direction is crucial in the layering technique to achieve an even deposition, otherwise peaking may occur where the middle of the printed surface keeps building at a greater rate than the sides. Although the goal of 700 microns was far from being achieved the progress made proved very encouraging, starting the second phase with a good working background.

From the outset of phase two it was realized that the number of prints required to reach the 700 micron goal, using the apparatus available, had to be decreased. To reduce the number of prints required the ink deposition per print had to be increased. The logical solution to this dilemma was to increase the stencil thickness as the deposit thickness is directly linked to stencil dimension. Several attempts were made to build up the thickness of the stencil by coating the screen with photoemulsion. Fourteen coats of emulsion resulted in a very opaque photostencil 0.5 mm thick that when exposed proved very difficult to process. The exposure of the emulsion was not being achieved due to its high opacity. A stronger bulb was tried but this resulted in the over-exposure of the top surfaces and again inadequate exposure of the deeper film. A maximum stencil thickness of 0.2 mm was achieved that was capable of being exposed and also produce sufficient detail. This stencil produced good results with ink deposits of 0.1 mm after drying. This method of stencil production was however very time consuming and not very accurate. An alternate stencil method was required.

The first breakthrough in the stencil production came with the use of a commercially available stencil that had a pre-mounting thickness of 76 microns. The stencil mounting

was very easy when compared to the layering technique tried previously and the exposure also proved to be much easier. Consistent results were achieved with successful prints of up to 400 microns thick in only 14 prints. Thus the number of prints required was reduced to 26 from the previous 41. It also became obvious that the use of a thick stencil with a multiple layering process was the most promising approach.

The 76 micron stencil was the thickest stencil available at the time and for this reason it was decided that attempts at producing a thicker stencil were left up to the project. Two methods were pursued with varied results. The first was to create a mold that would be used to form a thick stencil. Rectangular molds were made that had walls 3mm high. The mold was then filled with several brands of liquid photoemulsion, leveled off and left to dry. The result was a very uneven stencil with the inner section very thin and the perimeter substantially higher. Uneven evaporation of the solvent and surface tension had caused the inner areas to pull towards the outer edges. The amount of shrinkage experienced was also considerable. The outer edges had a total thickness of only 1 mm after starting at 3 mm. Attempts were made to add subsequent layers of the emulsion but these all failed, dimensional stability was unpredictable and subsequent layers caused bubbling in the base layers.

The second stencil manufacturing method that was attempted came as a suggestion from a Ulano, a major US stencil manufacturer [22]. Their idea was to laminate the 76 micron stencils that had been used previously to produce an even thicker stencil. The method of lamination was left up to the team. Several initial attempts failed and it did not appear that this would be practical. Persistence prevailed however and a successful lamination was achieved with two stencils. The result was a 150 micron thick stencil. The stencil was successfully mounted onto a screen mesh using liquid photoemulsion as the binder. The next obstacle was the exposure of the laminated stencil since there was no

previous experience on the process. An exposure regimen was developed bracketing the longest and shortest times anticipated. A development time was discovered and the stencil washed cleanly.

Printing with the thicker 150 micron stencil screen proved very encouraging. Print thicknesses of 0.12 and 0.16 mm were consistently achieved varying the pull speed, squeegee pressure, and number of flood strokes. Multiple prints were carried out and print thicknesses of 0.5 mm were achieved. The number of prints required to achieve this level was consistently 15. Registration became a problem once again. It was also decided to try a triple lamination in an attempt to reduce the number of prints required. The triple lamination ran into difficulties shortly after the third ply was layered on. It appears that when drying, the stencils off-gas. The sandwich created by the outer stencils prevents the gases from escaping, causing included bubbles. The size of the bubbles varied from pin holes to the size of a quarter. When exposed these holes caused distortions on the stencil and as a result the stencil was unusable. Various drying and laminating techniques were tried; all however produced the same results. The maximum stencil thickness that was produced using the lamination method was 150 microns.

All printing and stencil productions achieved to this point, although encouraging, had fallen short of the expected and required results. The thin stencil multiple layer method illustrated that multiple layering could work; the bonding to the grafoil substrate and the inter-layer bonding was better than expected for the ink mixture being tested. The problem with this method was the lack of adequate registration in the later prints. The built-up stencil proved to be a time consuming and difficult exposure option. For these reasons this method was abandoned. The thicker single and laminated stencils realized the best results, giving consistent stencil production and good printing results. The registration problem did however begin to surface once the ink deposition reached the 0.5 mm mark. Definite

reasons for this occurrence were unknown at the time and the thought on how to overcome the problem pointed to the stencil thickness and the printing apparatus.

To change the registration system, outside of purchasing specialized printing equipment, it was decided to modify the existing set-up. The printing base was left as it was now using a light spray tack glue to hold the substrate in place. The registration was realized by replacing the hinged mechanism with a vertical lift frame device. This device simply consisted of four metal rods positioned vertically on the printing base. The frame in turn had four metal cylindrical collars anchored in the frame at the appropriate locations such that the rods would pass through the collars with very little clearance. The frame was raised and lowered by hand and the off-contact distance was adjusted by inserting shims of a known dimension around the edges of the frame. Figure 5.1 illustrates the apparatus as it was constructed.

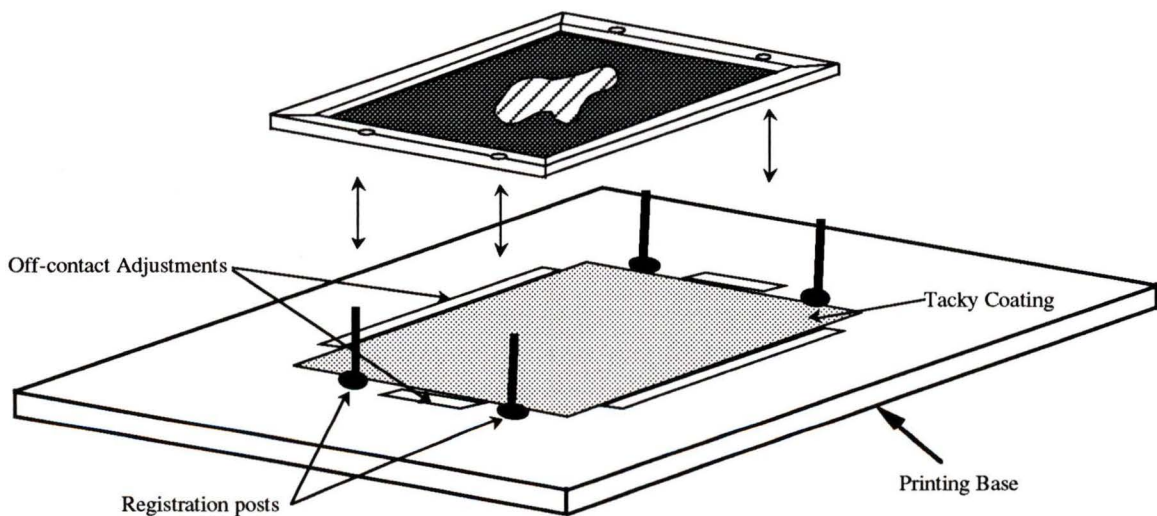


Figure 4.1: Printing Apparatus Constructed

Several prints with the new printing base demonstrated the improved registration system.

The issue of the stencil thickness, however, still needed to be addressed. Discussions with the major stencil manufactures throughout Canada, the United States and Europe failed to produce any solutions. The trend over the last twenty years was predominantly to produce thinner and thinner stencils. Industries like the printed circuit board manufacturing and fine arts printing all demanded that the stencils be as thin as possible to prevent the buildup of ridges between halftones. For these reasons the thought of finding a manufacturer of stencils thicker than 76 microns seemed doubtful. Speaking with our local supplier did however produce some encouragement. He had heard of someone in Calgary who was using a thick stencil for circuit work. Follow up on that contact led to the discovery of a stencil manufacturing company, Murakami, based in Japan. They were beginning production of thick stencils for the circuit industry. Just weeks before our contact the company had added a 400 and 700 micron MS thick film to its product line. Orders were sent out for both sizes.

Arrival of the Murakami MS thick film stencil material signaled the beginning of the final printing phase. Two screens were prepared, one with 400 micron and the other with 700 micron stencils mounted. Exposure tests for the 400 micron stencil revealed that using the 5kW Halide bulb the ideal exposure time was 5 minutes. The test patterns were developed with clean and crisp features indicating that pattern dimensions would not be a factor as they had previously been. Similarly the 700 micron stencils were shot and developed and the exposure time of 8 minutes proved to be ideal for sharpness and adherence to the mesh. Various mesh sizes were also tested for adherence and development. The larger mesh, 60, adhered well but did lose some detail when compared to the 86, 120 and 140 meshes. Printing tests would determine to optimum combination of stencil thickness, mesh size and number of prints required to build up the 0.7 mm channel heights.

Print tests commenced shortly after receiving new positive exposure acetates produced by a local blue printing shop. The first stencil tested was the 400 micron mounted on an 86 mesh screen. With the increased stencil thickness the use of flood strokes became more important than they had been with the thinner stencils. The flood strokes are done to fill the volume from the top of the mesh surface to the bottom of the stencil, or any amount within this range. Too much flooding would cause bleeding between the stencil and the grafoil and too little compromised the ink deposition thickness. Figure 5.2 illustrates the principle of flooding.

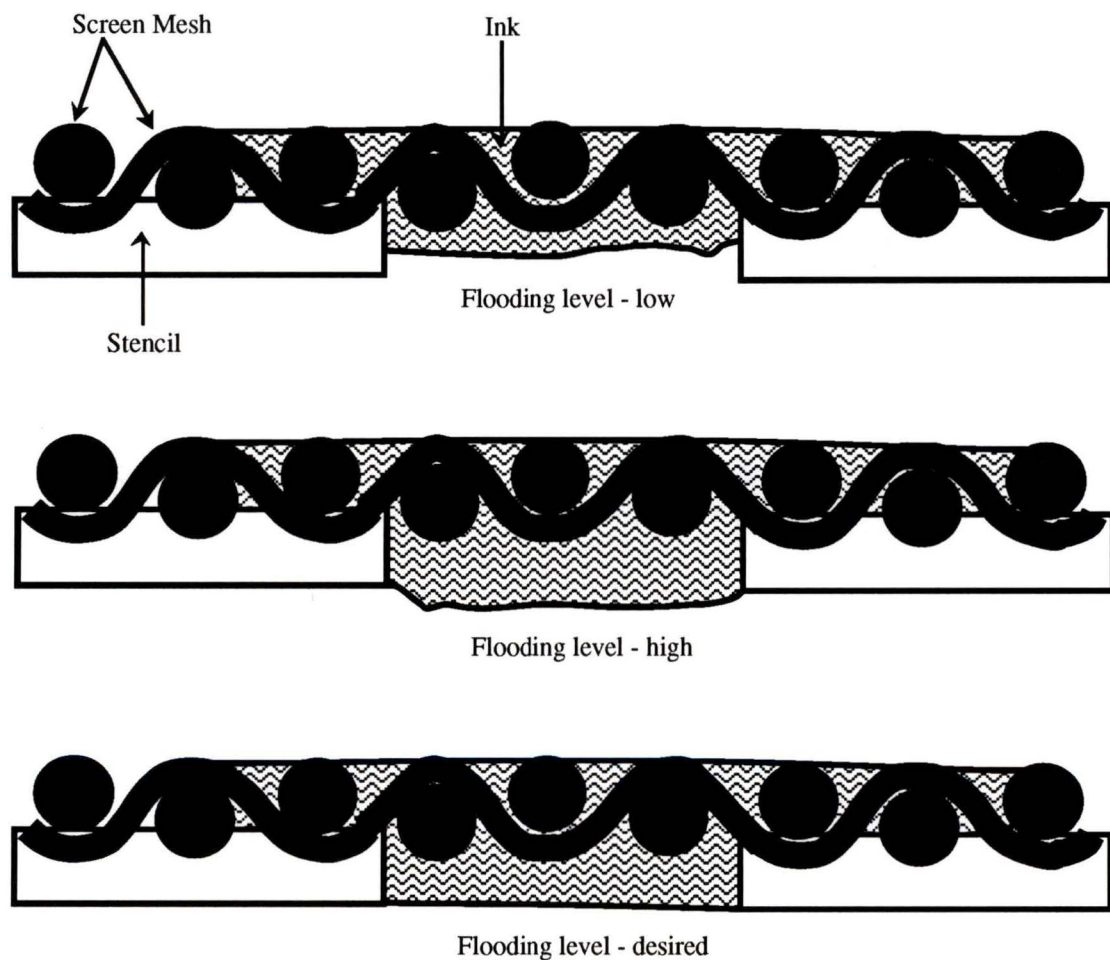


Figure 4.2: The Flooding Principle

With the 400 micron stencil fully flooded, the average wet ink deposit was 0.38 mm. Upon drying the ink deposit averaged 0.21 mm. Shrinkage amounted to almost 50 percent, but when compared with the first print thicknesses achieved, the deposits were now at least ten times thicker. The increased thickness did not affect the drying characteristics, no cracking, flaking, or loss of adherence to the substrate were observed, but air drying times were increased from several minutes to ten minutes.

When the second print was placed over the first the registration was excellent, adherence uncompromised but the combined dry print height was only 0.33 mm, an increase of only 0.12 mm. Figure 5.3 illustrates the proposed source of the uneven deposit thickness.

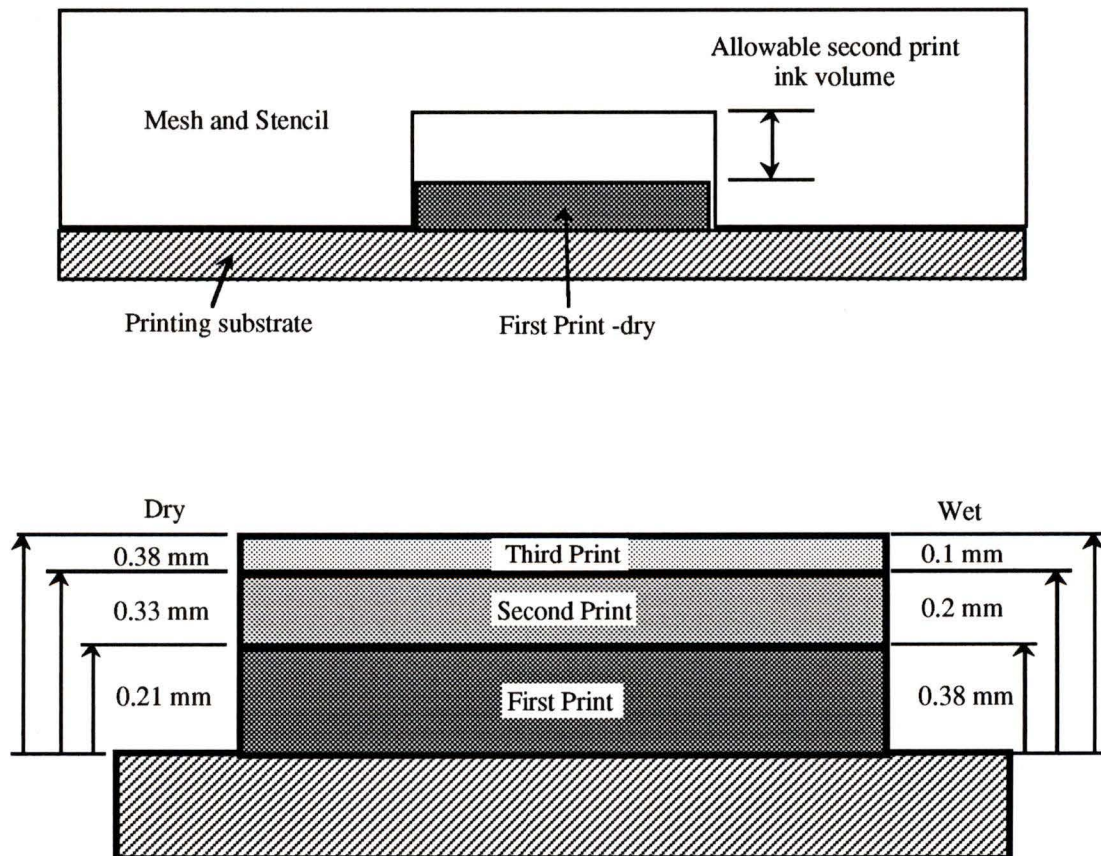


Figure 4.3: Deposition Thickness Theory Illustration

As illustrated in the previous figure, the height of the preceding dry print dictates the volume of ink that can be deposited on the next print. The alteration of the number of flood strokes now becomes important. If a fully flooded stencil is used with a high squeegee pressure the result is bleeding around the previous print and a loss of dimensional stability. The flood stroke must therefore be matched to previous print deposit to ensure clean and accurate prints. For example, the regimen followed with the 400 micron screen was: start with three flood strokes on the first print, followed by two flood strokes and finally one flood stroke on the final print. The maximum print thickness achievable using the 400 micron screen and the previous technique was 0.4 mm.

With the success of the 400 micron screen, the 700 micron screen was mounted and exposed. The washout process, removal of the unwanted stencil material, for the 700 micron screen was much more difficult, requiring not only more time but also more care to ensure that the stencil was not damaged. After careful processing the screen was put into use and printing was carried out. First print wet ink deposits averaged 0.7 mm, consistent with the previous 400 micron stencil results. The dried thickness was 0.35 mm once again illustrating the 50 percent shrinkage of the ink being used. Subsequent prints demonstrated similar properties as the previous stencil and the 0.7 mm dry print thickness was built-up after a total of 7 prints. The goal of building up a 0.7 mm thick screen printed flow field plate was achieved.

The possibility of producing a thicker print initially seemed unlikely without a thicker stencil. Discussions with Murakami, the stencil manufacturer, indicated that thicker stencils were possible, although difficult, and that they had actually produced a 1000 micron stencil but as of yet there was no market demand for such a thickness so it was not commercially available [23]. Techniques of producing thicker prints without thicker stencils were discussed with the Art Department. One possible solution would be to vary

three of the printing variables: off-contact distance, squeegee pressure, and flood stroke. Varying the off-contact distance and the squeegee pressure such that the bottom of the stencil came just below the surface of the previous print may allow a thicker ink deposit. This however would require the ability to measure and control the squeegee pressure and the off-contact distance, characteristics that our set-up did not have and would have had considerable cost implications.

Throughout the printing tests, several other process issues became evident and were dealt with. One problem that plagued the printing for quite some time was the sticking, on occasion, of the stencil to the grafoil. Upon release graphite particles would be stuck to the stencil and the cleaning of these particles proved very difficult. At the same time the standard ink formula appeared not to have the same flow characteristics and had increased tackiness even though the exact same ingredients, proportions, and mixing methods had been used. It was discovered that all these occurrences were linked to the humidity. On days when the humidity was high, the stencils apparently absorbed some moisture and became sticky enough to pull up some of the grafoil surface. Similarly the humidity affected the ink composition, changing the viscosity slightly. To solve these process issues two steps were employed. The stencil was given a light spray coating of a teflonated mold release material prior to carrying out any printing. The condition of the stencil was then monitored throughout a printing run and at any time when the stencil appeared to become tacky, the mold release was reapplied. One application was typically sufficient for one entire plate production. If after the mold release was applied, the ink still exhibited unacceptable tackiness an additive known as an extender was added to the mixture on an as required basis (the amount depending on the days relative humidity, a few drops per 250 ml ink mixture typically). The extender effectively thins the ink slightly and extends the drying time of the ink formula allowing for unhindered printing without changing the overall ink composition significantly.

The inclusion of humidity controls into a manufacturing plant would be a costly addition to the process, but there are alternatives. Since the application of the mold release spray did not affect the performance of the inks on low humidity days, this step could be incorporated for all printing operations for a much lower cost than a plant humidity control system.

The pull angle of a screen refers to the angle the squeegee makes with the principle components of the stencil. It was discovered that the pull angle has a large influence on the resultant print when using thicker stencils. When the squeegee is parallel to the major components of the stencil, the effect is similar to pulling a squeegee across a washboard. The chattering of the squeegee causes a ripple effect and results in an uneven ink distribution and inaccurate registration. The surface of the ink deposit was noticeably rippled and some areas of the stencil did not deposit any ink at all. The solution to this problem was to alter the stencil orientation on the screen by placing the desired shape's primary angles as perpendicular to the squeegee pull as possible. Figure 5.4 illustrates this principle. Careful orientation of the pattern solved this problem in subsequent prints.

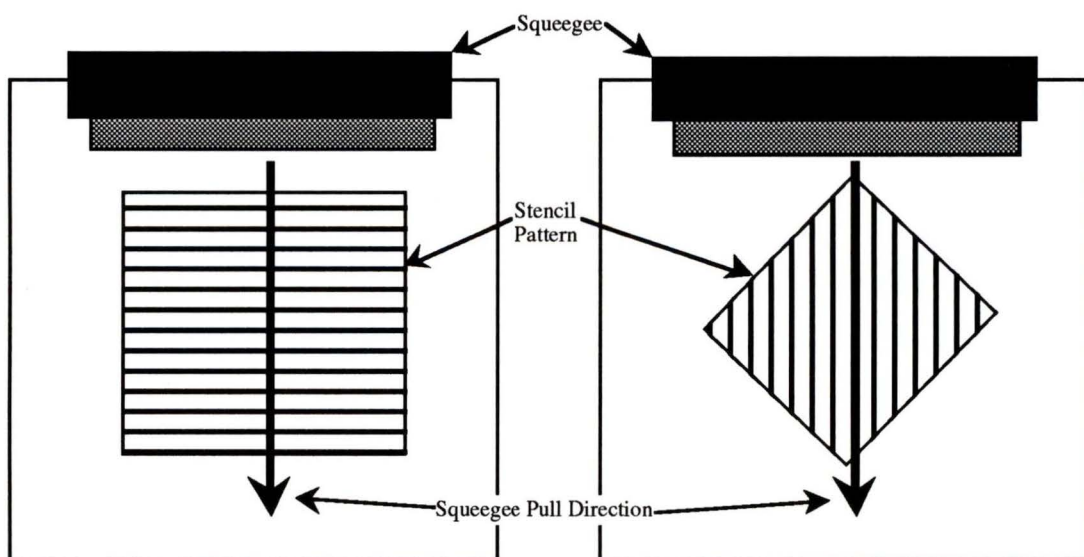


Figure 4.4: Squeegee Pull and Stencil Angle Relationship

The size of the frame and the screen mesh tension also affected the printing results of the thicker stencils. The use of a large frame to support a proportionately small stencil translated into the mesh not having sufficient tension to create a large enough snap-off force (the elastic tendency of the screen mesh when the squeegee pressure is applied). This resulted in the mesh not lifting off of the printing surface as was discussed in the off-contact section. The solution was to increase the off-contact distance, but this resulted in large deformations in the mesh with the increased squeegee pressure required to achieve stencil-substrate contact. These deformations produced an image with insufficient dimensional stability to be of any use. At the other end of the spectrum, the use of too small of a frame for a specific stencil required a large squeegee pressure as well, only this time to overcome the taught screen around the periphery of the frame. The result was an uneven squeegee pressure distribution across the surface of the stencil, affecting overall print quality. The selection of the ideal frame size coupled with the proper mesh tensioning produced far superior results.

4.2 Ink Development

Occurring concurrently with the printing technique development was the investigation into providing a suitable ink that would satisfy all of the technical requirements of a fuel and oxidant delivery plate in a fuel cell. Briefly stated, these requirements are: chemical stability in the fuel cell environment, structural integrity and good conductivity. The chemical stability refers specifically to the ink not contaminating the membrane with positive ions resulting in impaired membrane performance and not allowing the leaching of ions into de-ionized cooling water possibly causing electrical shorts. Sufficient structural integrity translates to the ability to withstand the compressive forces required to maintain the stack form and provide sealing, all while exposed to the fuel

cell environment. Conductivity refers to the quantity of electricity transferred across a unit area per unit potential gradient per unit time.

To test the chemical stability would require the exposure of the ink material into a functioning fuel cell followed by testing and evaluating the cooling water and the MEA. This option was not available so the best substitute was to consult with Dr. Steve Holdcroft, the head of the NGFT electrochemistry group at Simon Fraser University. Even this however was not a perfect substitute for actual field testing of the materials because the constituents of the ink bases were, for all commercially obtained samples, proprietary knowledge. Only the basic solvents used in these inks could be assessed. For these reasons the evaluation of the chemical stability was left for future testing.

The structural integrity of the inks, on the other hand, was easily evaluated. The test consisted of hanging a standard (3 cm x 1 cm x 0.25 cm) grafoil strip coated with the material in a humidity chamber and exposing it to temperatures of 100°C and 100 percent humidity for an eight hour period. The samples were allowed to cool to room temperature and then put through the cycle once more. Following the second exposure, the samples were removed from the chamber and several observations noted while still hot. The first observation was of the general surface and specimen condition. Checks were made for pitting, adherence to grafoil, cracking or other deformations that would indicate that the sample was under any undue stresses. The flexibility of the sample was also examined under the assumption that if the material became very soft and flexible it was unlikely to be able to withstand the compressive forces of the stack and maintain the required channel profile. Likewise if it was too hard and brittle it would most likely crack with thermal cycling. Table 5.1 lists the sample materials that were tested in the humidity chamber.

Table 4.1: Humidity Test Chamber Materials and Results.

Sample	Supplier	Pitting	Cracking	Flexibility	Adherence	Evaluation
WB 5101	TW Graphic	no	no	medium	excellent	suitable
LTX 117G	Masterbond	yes	yes	soft	good	suitable
Oxycast 100	Oxychem	yes	yes	medium	poor	not suitable
F113	Tracon	no	no	brittle	good	suitable
TD 2979	Tracon	no	no	soft	poor	not suitable
TD 2958	Tracon	no	no	soft	poor	not suitable
CEA 155	IPN	yes	yes	brittle	poor	not suitable
X5G	Masterbond	no	no	medium	good	suitable

Of the eight ink base materials tested only four exhibited favorable exposure characteristics. The material that performed the best was the commercially available water based ink WB5101. It exhibited the best adherence and flexibility combination.

Along with the ink specimens, the grafoil was also observed under the exposure conditions. The samples of grafoil exhibited no adverse reactions to the environment. No swelling or delamination occurred.

4.2.1 Conductivity

Next to the proof that screen printing was a viable concept, the second most important goal of the thesis was to develop a conductive ink that could be used with screen printing. The bulk resistivity of the Ballard MK V plate, 10^{-3} Ohm-cm, was used as the high target for the ink with acceptable levels being one order of magnitude greater, 10^{-2}

Ohm·cm. Several options presented themselves as possibilities and it was decided to investigate the following paths:

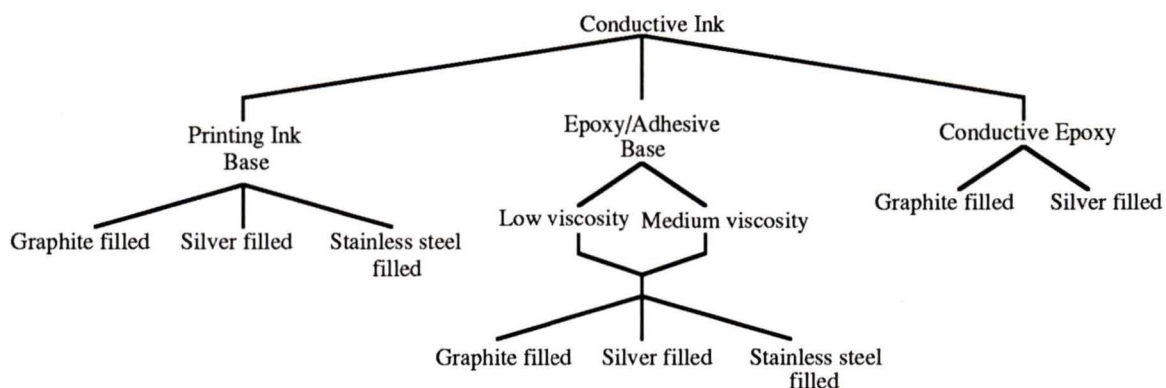


Figure 4.5: Conductive Ink Options

With each of these options the amount of filler added to make the carrier conductive was varied from none to the maximum amount allowable for the ink to remain printable.

The test methods used were based on the Van der Pauw technique, which is “a method for measuring specific resistivity and Hall effect of discs of arbitrary shape.” The circuitry set up followed the outline illustrated in Appendix A [24]. The use of this technique assumes that the sample is flat with small electrodes located along the edges. Sample preparation consisted of modifying sample holders used for polishing and etching materials such that they can be viewed under a microscope to inspect grain boundaries and other structures. The holders were shortened and four slots cut into the side walls for the insertion of wire leads prior to curing. After the samples were hardened they were removed from the holders and the top surface flattened using a sanding disk. The result was a flat disk approximately 1 mm thick with flat parallel surfaces.

To evaluate the resistivity, a voltage is applied (the value of which depends on the material properties) and the resultant current flow is measured. The procedure is repeated

for each of the different position numbers (as seen in Appendix A). Once the four measurements are taken, the current is reversed and the measurements taken again. The ambient temperature does not effect the results, but the temperature of the sample may rise if the applied current is too high. Thus the tests were conducted using minimal voltages and readings were taken rapidly. With the readings taken, the resistivity, ρ , of the sample was calculated using the following [24]:

$$R_{1,2-3,4} = \frac{(V_3 - V_4)}{I_{2 \rightarrow 1}} \quad (5.1)$$

$$R_{2,3-4,1} = \frac{(V_4 - V_1)}{I_{3 \rightarrow 2}} \quad (5.2)$$

$$\rho = \frac{l\pi}{\ln 2} \left[\frac{R_{1,2-3,4} + R_{2,3-4,1}}{2} \right] f \quad (5.3)$$

Where t = thickness of the material and f is a correction factor which takes into account the shape of the sample.

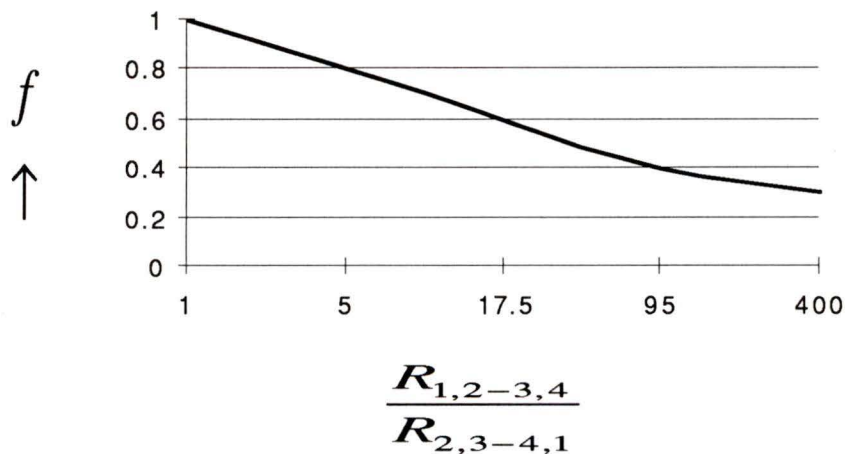


Figure 4.6: Van der Pauw Correction Factor f

4.2.1.1 Conductivity Results

A standard test specimen was used to calibrate the test rig. A piece of a Ballard MK V coolant delivery plate was cut and placed in the assembly. The sample tested consisted of a square plate measuring 2 cm x 2 cm and having a thickness of 0.5 cm. The Ballard plate exhibited a resistivity of 9.06×10^{-3} Ohm-cm. This value compared well with the Ballard estimation of 3.5×10^{-3} Ohm-cm.

The following table is a list of the samples that were tested using the above apparatus illustrating the base materials and the fillers used and in what proportions.

Table 4.2: Conductive Ink Mixtures Tested

Base Material	Weight % Filler					
	0	10	30	50	70	90
WB5101						
Graphite Flour 0-53 microns	x		x	x		
53-75 microns	x		x	x		
75-150 microns	x		x	x		
WB5101						
Silver powder	x		x	x		
WB5101						
Stainless steel powder <100 microns	x		x	x	x	x
F113						
Graphite Flour 0-53 microns	x		x	x		
53-75 microns	x		x	x		
75-150 microns	x		x	x		
F113						
Stainless steel powder	x		x	x	x	
F113						
Silver powder	x		x			
X5G	x					
LTX117	x					

Of the above samples the X5G and the LTX117G were the only commercially available “conductive” epoxies that were tested. Their typical application is in the mating of conductive surfaces with minimal epoxy thickness. WB5101 is a commonly used ink base

in the screen printing industry. It is water based and contains no fillers. Other than basic solvents listed on the material safety data sheets (MSDS) the remaining ingredients were proprietary. When considering epoxies to test as bases the ability to withstand the environmental conditions and the viscosity were of primary importance. Of the epoxies obtained and tested in the humidity chamber the only one to exhibit desirable qualities was Tracon F113. The F113 also had a very low viscosity, 180 centipoise (cps), when compared to other epoxies available.

The test carried out revealed that none of the base materials that were being used exhibited any conductivity on their own once their solvent or water based carriers had been completely driven off. This result was anticipated as a search done prior to material selection into conductive bases, revealed the same outcome. The two conductive epoxies tested did not achieve the same resistivities that were specified in their technical data sheets. The Master Bond X-5G stated resistivity was 7-8 Ohm-cm, while the tested result was 200 Ohm-cm. Similarly the LTX 117G had a rated resistivity of 5 Ohm-cm and the tested value was 178 Ohm-cm. These results were considered disturbing until it was realized that these adhesives are typically applied (and ratings produced) with only 1 mil thickness while our samples were nearly 1 mm thick. The thickness of the deposit greatly affected their conductive performance.

Following the tests of the ink bases, the same bases excluding the X5G and LTX117G were subjected to the addition of graphite, silver, carbon black and stainless steel powders. The graphite particles that were added were made from artificial graphite and had been sifted into three sizes from a common stock. The sizes used were 0-53 μ , 53-75 μ , and 75-150 μ . These sizes were chosen in conjunction with the mesh sizes that

were being used to test the screen printing. The use of larger particles was precluded by their clogging the screens and not allowing smooth pulls. WB5101 and F113 were both mixed with the various graphite sizes in the proportions listed in Table 5.2 .

The F113 and graphite samples all exhibited resistivities of a perfect insulator. This was not an expected result and the cause for the lack of conductivity was unknown at the time. After discussions with Walter Merida regarding packed particle bed theory and work that he had done, it was concluded that the epoxy resin effectively coated the graphite particles creating a protective barrier around each particle and not allowing any contact amongst the particles which would have allowed for conductance. Tests with the stainless and silver powders confirmed these results. The F113 epoxy was not a suitable base for a conductive ink.

Using the water based ink produced much better results. The graphite flour fillers produced the best results of the three filler materials tested. Table 5.3 illustrates typical resistivity results achieved with the WB5101 and graphite flour mixtures.

Table 4.3: Sample Resistivity Results

Resistivity Ohm cm		
Base Material	Weight %	
Filler	30	50
WB5101		
Graphite Flour 0-53 microns	1.19	2.4
53-75 microns	0.79	1.09
75-150 microns	0.65	0.92

These results show two trends: the resistivity of the sample decreases with the lower loading amounts, and the resistivity also decreases with the increase in the particle size. Neither of these observations were expected, in fact initial predictions were of the opposite nature.

The next sample tested was that of the water based ink coupled with the stainless steel particles. Initial mixtures of ink and particles were made with weight percents of 30, 50, 70 and 90. Surprisingly none of the samples registered any conductivity. One possible reason for the lack of conductivity was the existence of an oxide layer on the particles. A series of samples were subsequently etched in Miller's reagent and mixed immediately with the ink base. The resultant ink mixtures once again failed to exhibit any conductivity. It was surmised that the mass of the stainless particles was too great for the base to hold in suspension and this resulted in settling of the particles leaving the insulating base at the surface.

The final filler tested with the WB5101 base was the silver powder. Two samples were prepared with 30 and 50 weight percent ratios. The results of the tests indicated that the samples were marginally conductive with resistivity measurements of 75 Ohm·cm, considerably short of the goal and at a considerable increase in price over the graphite. Although silver is more conductive than graphite the shape of the particles must influence its electrical properties. The silver powders consisted of spherical particles whereas the graphite particles are ragged flakes.

The results discussed up to this point indicate several aspects of filler properties that are desired when formulating a optimum conductive recipe. The particle size, shape, and distribution all affect the conductivity as does the viscosity of the ink base. When considering the viscosity, the tests illustrated that too low a viscosity allows the particles to become thoroughly coated effectively acting as an insulator. The ink must also exhibit sufficient viscosity to actively suspend the particles and not allow settling which results in the formation of an insulating skin on the ink surface. Further investigation of the particle size and distribution was required to understand the mechanisms at work and their

influence on conductivity. For this reason it was decided to get a closer look at the microstructure of the ink mixtures tested.

4.2.2 Microstructure

Investigation of the microstructure was carried out with the use of a confocal microscope. The microscope was located in the Biology Department at UVic and Dr. Burke generously donated his time in assisting the investigation. Briefly, a confocal microscope makes use of a variable frequency laser which can be focused at various depths within a substance. The energy of the laser causes material to fluoresce and the light produced is captured by a computer. The laser cycles through a series of depths recording information for each layer. The layers are then combined by computer and the result is a three dimensional picture of the material. This technique was useful since it was non-destructive in nature and allowed a look at the internal microstructure of the inks.

Sample preparation consisted of mixing a fluorescing material in with the ink and spreading a thin coating onto a glass slide. The fluorescing material used was Rhodamine B. The amount of Rhodamine added was 0.001 percent by volume. Two sets of samples were prepared for investigation. The first set consisted of the water based ink mixed with carbon black 30 weight percent, graphite 30 and 50 weight percent, and silver powder 30 weight percent. LTX117G, and X5G samples were also prepared to investigate particle size. The second set of samples prepared was identical to the first with the exception that these samples were heat treated at a temperature of 150°C for 60 minutes after initial curing. This was done to see if heat treatment would have a result on the structure.

The LTX117G and X5G and carbon black samples failed to produce any results due to the opacity of the mixtures. The silver powder sample revealed a particle size

distribution of 5-10 μ in diameter with the particles being spherical. Each particle appeared to be coated by ink base with small clumps dispersed throughout the matrix.

The graphite mixtures provided the best and most interesting results. On the first set of slides there existed a thin skin on the surface. This indicated that a certain amount of settling had occurred. A set of slides were prepared by screen printing the ink onto the surface and the outcome was the removal of the skin. This would theoretically improve the conductivity. Figure 5.8 illustrates two confocal microscope pictures. The RHO1deep sample consisted of graphite particles ranged from 53-75 μ in size and a 30 weight percent ratio. The 'deep' indicates that this picture is of a depth >20 μ form the surface. RHO3deep was a sample whose graphite particles were less than 53 μ in size and also mixed at a 30 weight percent ratio.

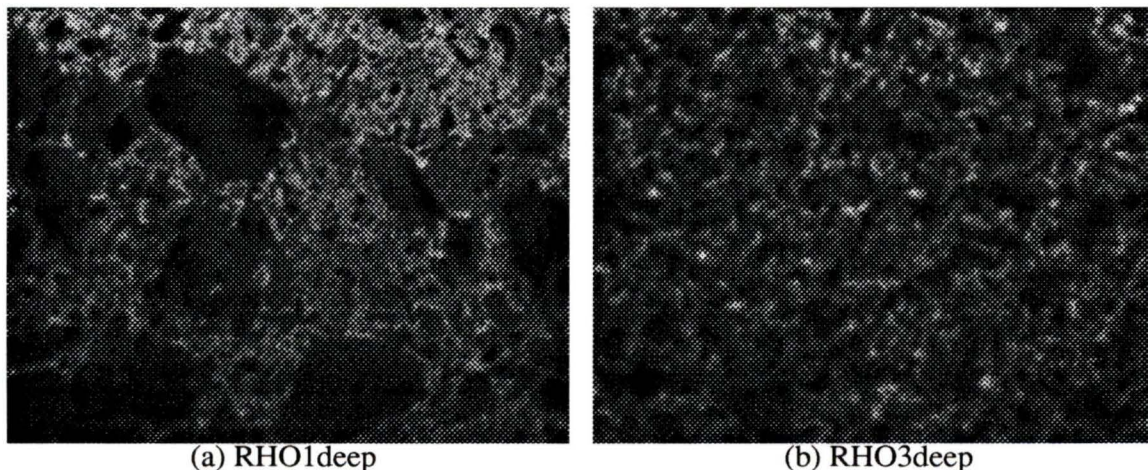


Figure 4.7: Confocal Microscope Pictures of (a) 30 weight percent Graphite, 53-75 μ Particle Size in WB5101 (b) 30 weight percent Graphite, <53 μ Particle Size in WB5101

Of particular interest to note with these pictures is the difference in dispersion of the graphite particles. Both samples were mixed identically and prepared on the slides in the same manner. In the sample containing the smaller particles they appear to be dispersed

much more evenly and at regular intervals. The larger particle mixture, on the other hand, contains clumps of graphite that come in contact with other clumps. Figure 5.7 (b) demonstrates the reason the F113 Epoxy failed to produce any conductance at all and had a higher resistivity than the other sample (a). The individual particles appear to be coated by the ink base effectively isolating them from their neighbours electrically. The other sample in Figure 5.7 (a) shows the existence of a network or a connected pathway of graphite particles which permit easier flow of electrons. This, it is felt, is the source of the improved conductance of the samples containing larger flake particles, an important discovery. The use of larger flakes requires the use of larger mesh counts for the screen printing process which may effect the adherence of the stencil material to the screen.

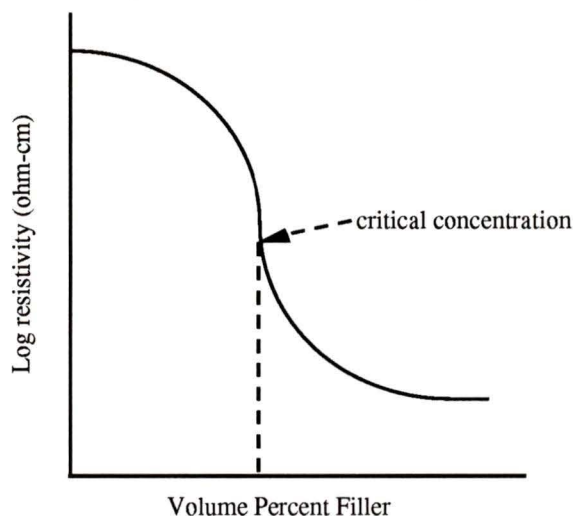
4.2.2.1 Percolation Theory

The above discussion attempts to deal with the question of particle size and distribution, but what it does not address is the loading issue coupled with the size and distribution. Percolation theory was suggested as a means to investigate the optimum loading conditions for a conductive particle in a matrix. The trend illustrated in the resistivity tests performed suggested that the samples with higher loading actually had higher resistivities than those of lower loading. This seemed counter intuitive so the investigation into percolation theory was launched.

Simply stated, percolation theory describes the movement of a classical particle through a randomly distributed medium [14]. Traditional percolation theory is concerned with the flow of “fluid” between the nodes of a regular lattice. The randomly dispersed filler particles of a conductive composite represents a classic percolation problem. According to Gurland [15] the bulk resistivity of a metal filled polymer varies with filler concentration. Below a certain concentration the resistivity of the composite is virtually the

same as that of the matrix. As the filler concentration is increased it reaches a critical concentration after which the resistivity of the composite drops drastically. Figure 5.8 illustrates this principle [15].

Figure 4.8: Universal Shape of the Resistivity versus Filler Loading Plot.



In a percolation model a method known as the Monte Carlo simulation method is used [14]. A conductive composite is first represented by a set of randomly located sites deposited in a unit cube by a pseudo random generator. Each site can represent a sphere of a given size inside the cube. The program checks to determine if any of the spheres overlap indicating a bond. With all the bonds established the program then checks for a continuous path from one side of the matrix to the other. If a path exists the system is said to percolate indicating that electricity would conduct. The size of the spheres is then altered and the test for percolation repeated. This process continues until the sphere size that represents the transition between percolation and no percolation is determined. This represents the percolation threshold. Because the percolation threshold is determined by the particle size and not the number of particles it is termed the critical area fraction. The accepted critical area fraction for the spherical shape is 68 percent [14]. This value drops drastically if the shape of the particle is rectangular. With the rectangular shape the aspect ratio becomes an

important characteristic. The higher the aspect ratio, the lower the critical area fraction. Table 5.4 illustrates these results [14].

Table 4.4: Critical Area Fraction as a Function of Aspect Ratio

Aspect Ratio	1	5	10	20	50	100
Critical Area Fraction	68%	45 %	33 %	21 %	9.5 %	5.3 %

These results indicate that it is not the weight percent of the filler used that dictates the resultant conductivity of the matrix, as was initially surmised, it is the volume percent and the particle shape that are the overriding factors. In the samples tested previously and shown in table 5.3 it was concluded that the resistivity decreased with the lower loading rates by weight and also the increase in particle size. The relationship between weight percent and resistivity previously discussed is therefore inconclusive. The subsequent relationship of particle size and resistivity, however, is validated by percolation theory and the test results. The use of high aspect ratio, irregularly shaped and randomly distributed conductive particles, at or above the critical area threshold, would achieve the best possible conductivity. These conclusions are also supported by the results obtained in the microstructure study.

4.2.3 Cost Analysis

The overall rating of the success of the project comes down to the satisfaction of the three initial criteria: use of screen printing as a viable technique to manufacture flow field plates, adequate conductivity and overall cost of manufacturing savings. The issues of screen printing and conductivity are discussed above. When considering the cost of manufacturing of a screen printed bi-polar plate two levels were considered. The first level was the material costs. These costs were tangible and were readily calculated as seen

below. The manufacturing costs, however, were much more difficult to calculate. They had to include the process costs, and capital costs.

4.2.3.1 Material Costs

Material costs were broken down into two separate categories, the ink base and the substrate. Included in the ink costs were the ink base and the filler material. The price quote provided by TW Graphics for mass quantity purchase of their WB5101 ink base was \$6.50/litre. The amount of ink base used for each plate averaged approximately 50 ml. This translates into a per plate cost of \$0.32. The graphite flour used as the filler had a bulk cost of \$1.50 per pound or \$3.30 per kilogram. The amount of graphite used per plate averaged 60 grams. This translates into a graphite flour cost of approximately \$0.20 per plate. The cost of the grafoil depended on the thickness and grade used. Retail price quotes from Union Carbide for their nuclear grade grafoil are illustrated in Table 5.5. They would not give a quote for large volume purchases but it can be assumed that these prices are above what could be expected.

Table 4.5: Union Carbide Grafoil Premium Nuclear Grade Retail Price Quotes

Thickness	Price per Roll	Price per Plate
0.015"	\$840	\$1.87
0.010"	\$634	\$1.41
0.005"	\$475	\$1.05

Summation of the individual costs results in a per plate material cost of \$1.57-\$2.39. The raw material cost of a Ballard plate, as stated previously, was \$20. A ten fold savings could be achieved in materials alone.

4.2.3.2 Process Cost

To determine the process cost the process first had to be envisioned. The availability of grafoil as the printed substrate lends itself to an assembly line-type process since it is available in large rolls and is flexible, similar to paper. Whether the manufacturing of the plates was to be batch or mass production would determine the scale of the operation. Figure 5-9 illustrates one possible process configuration.

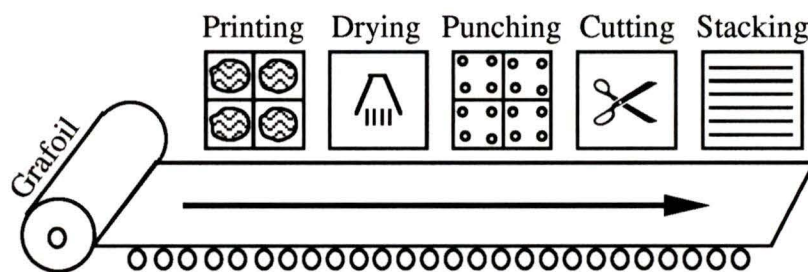


Figure 4.9: Screen Printing Bi-polar Plate Process Configuration

Compared to the CNC approach of manufacturing a bi-polar plate, the screen printing process illustrated above would have the benefits of higher production rates, lower capital costs, and reduced labour costs. The degree to which these advantages would reduce the overall manufacturing cost is unclear. Considering the reduction achieved by the material components and the fact that batch and mass production generally reduce production costs 10-20 times [10] it is safe to estimate that the \$80 CNC manufacturing cost would be reduced to \$3-\$5 per plate with screen printing. This results in an overall per plate cost of \$4.37-\$7.26.

Chapter 5

5. Conclusions and Future Work

5.1 Conclusions

5.1.1 Process Feasibility

The thought that a 0.7 mm (channel depth) flow field plate could be produced by screen printing techniques was met with much skepticism. In the end, however, the doubts were pushed aside as the goal of achieving a 0.7 mm thick screen printed flow fields of the required detail was produced. The technique for producing such a plate underwent countless renditions and modifications until the preferred process of utilizing a thick 700 micron stencil coupled with multiple layer printing achieved the desired results. Process feasibility was perhaps the most significant result achieved.

The apparatus that provided the best results in terms of registration and off-contact adjustment made use of a vertical lift mechanism by which the frame was raised vertically on three rods attached to the printing base. This resulted in accurate alignment of the screen and frame that allowed for subsequent deposits to be accurately aligned on the previous layer.

Other process issues which affected the print deposition and sharpness of detail included screen tension, frame dimension, squeegee pressure angle and pull speed, and the stencil to squeegee pull orientation. Screen tension and frame dimension define the snap-off characteristic of the particular screen and as such determine the ideal off-contact

distance. The thicker the ink deposit the larger the off-contact distance required and therefore the greater the screen tension needed.

The squeegee angle, pressure and pull speed all proved critical for the print outcome. Measurement of these variables was not an option with the apparatus used, as such the technique developed relied on the feel of the printer for process repeatability. The angle of the pull stroke to the major stencil detail also proved critical for maximum and even ink deposit. When oriented perpendicular to the major stencil detail the squeegee would pull smoothly and the resultant ink deposit was thick and even. Parallel orientation of the squeegee and major stencil detail resulted in a chattering or washboard effect. The ink deposit demonstrated uneven thickness and a rippled surface.

The use and regulation of flood strokes was also a key component in achieving a good ink deposit. The first and second prints required full flooding while the amount of flooding was reduced with each subsequent print. Over flooding results in bleeding and an under flooded screen does not optimize the printing capability requiring more prints to achieve the desired result.

5.1.2 Ink Conductivity and New Research Directions

The goals set out for conductivity in the invention memo [27] and the initial project outline have not yet been achieved, but a good understanding of the contributing factors was realized and the results were not far from the target. Initial results demonstrated that commercially available conductive graphite epoxies performed poorly when applied outside of their intended application. Their high solvent contents caused cracking and flaking when these adhesives were applied thicker than the recommended 1 mil.

The next approach was to use conductive filler particles suspended in an ink base. Through investigation into percolation theory it was concluded that the use of high aspect ratio, irregularly shaped, randomly distributed conductive particles at or above the critical area threshold gives the best resistivity results. The size of the particles also influenced the conductivity results. The larger the flakes the higher the conductivity. This relationship supported the percolation theory of increasing the volume percentage of the filler. The use of a confocal microscope enabled investigation into the microstructure of the inks being tested. It revealed that low viscosity epoxy mixtures tended to coat the individual particles effectively insulating them and preventing the transfer of electrons.

The use of metallic particles, silver and stainless steel, exhibited the existence of oxide layers on their surfaces. Removal of these oxide layers by chemical etching prior to mixing in the inks proved difficult, and the results were less than inspiring for further attempts. Their cost was also a deterrent to their continued use.

The ink base that proved to be the most useful, exhibiting flexibility of application was the commercially available water based printing ink WB 5101. This ink allowed varied loading of filler materials while still maintaining its print qualities.

Although the target resistivity was not achieved, it was concluded that the bulk resistance of the printed ink was not the greatest contributor to the conductivity problem of an assembled stack. Research by another NGFT member, David Leboe, suggests that the contact resistance between the various layers within the fuel cell stack pose a larger hinderence to the overall stack conductance than does the results achieved with the conductive ink [25]. This, however, does not remove the requirement for a highly conductive ink, it just relieves the success/failure label attachment based on the conductivity alone.

The discovery of the influence of particle size and distribution within the substrate with regards to improving conductivity proved significant in the challenge of understanding the conductivity issues. Investigations into ink microstructure and percolation theory coupled to illustrate what makes a good conductive ink and opens the door to future paths of investigation into achieving the rigorous demands of a screen printed fuel cell plate. These discoveries will aid in the development of a highly conductive low cost printing ink suitable for use in the fuel cell.

Overall the project provided challenges in a multi-disciplined way that, as a whole, were met and the results achieved significant. The ability to manufacture a flow field plate for use in a PEM fuel cell stack for under \$10 a plate is a significant achievement. Screen printing even lends itself to batch production and mass production processes, exhibiting easy scale-up potential. When compared with current manufacturing techniques, screen printing also offers the ability to rapid prototype. Flow patterns can be changed, flow channel dimensions altered and plate geometry's modified requiring only a matter of hours to produce functioning prototypes.

5.2 Future Work and Recommendations

The successes achieved in the development of a screen printing technique for the low cost manufacture of a PEM fuel cell flow field plate serve the purpose of inspiring further development and refinement of the process. These further developments would demonstrate the batch and mass production applications of the techniques developed and lead to the acceptance of these techniques as a viable manufacturing method. Future development in the areas of printing process and ink conductivity are recommended.

5.2.1 Screen Printing

The printing process developed was in a sense rather crude in that all the printing was all manually performed. Refinement of the process could easily be achieved by automating the squeegee pressure, angle, pull speed and off-contact distance. This would take the guess work out of these variables and not rely on the operators talents to the same degree. Automated machines of this nature are readily available and reasonably priced. Construction of such an apparatus may also provide a good undergraduate design project.

To increase the thickness of the ink deposit on a per print basis several options present themselves. Thicker stencils could possibly be produced but as of yet they were not available. Stainless steel mesh material is made up of smaller diameter wire than the synthetic material screens increasing the open volume percentage of similar mesh count screens. Using the stainless steel mesh would permit the passage of greater volumes of ink for a given mesh count.

Consistent with the results that larger, high aspect ratio particles provide increased conductivity the use of larger meshes and the stainless screens would provide the passage of these particles. At the same time, however, the maximum mesh count of the screen is determined by the required detail of print and the ability of the stencil to adhere to the screen. Optimization of these variables is required for the production of satisfactory plates.

The use of a UV curing ink is another option that presents itself for the building up of thick prints. Conventional inks consist of 30 percent-50 percent solids and 50 percent-70 percent solvents which evaporate upon drying leaving only the 30 percent-50 percent of the printed ink on the substrate. UV inks however use no solvents, since the ink becomes a solid by photochemical reaction and not evaporation. Therefore the ink which is printed remains 100 percent solid on the substrate. The end result could be a 700 micron thick

channel in only one print. Drying times for the UV inks are under one second compared to the 4-5 hours required to produce the same thickness using conventional inks. This would enhance production rates and most likely offset the increased capital, ink and operating costs.

The screen printing process is a versatile technique that allows for easy modification of not only the patterns but also the materials used for printing. Different materials can easily be printed at different locations on the substrate to vary the plate characteristics. The porosity of the printed surface can be altered by using different ink base materials and follow-up processing. Heat treatment, for example, could be used to increase the porosity of the deposit resulting in an increase in the active area and power output. Outer areas could subsequently be made non-porous to ease the sealing problems. The possibilities are only limited by the ingenuity of the user and availability of materials.

5.2.2 Ink Conductivity

The conductivity issue as described earlier was a difficult portion of the project. On the one hand the best conductivity possible was desired for the printed ink to reduce the overall ohmic losses occurring in the fuel cell stack. Conversely the discovery that the contact resistance between stack components was of greater concern than individual conductivity's, relieved some of the pressure to produce the best conductive ink possible. With this said the production of the best ink possible was still of major concern and a concerted effort was made to improve the conductivity situation. Several ideas presented themselves throughout the development process to enhance both the inks conductivity and reduce the contact resistance.

Continued research into increased particle size, aspect ratio and distribution are considered optimistic alternatives for increasing ink conductivity. Concurrent with these investigations, the adaptation of the screen printing process must also occur to accommodate the changes in ink materials. The introduction of a conductive ink base would also increase the overall conductivity of the ink. At present the ink's conductivity relies solely on the particles suspended within. Alternative ink base materials could potentially solve the conductivity problems.

Several options for dealing with the contact resistance issue were also developed throughout the project. Sprinkling dry graphite particles on the still wet surface of a printed plate would present good contact surface for the mating MEA, overcoming the insulating tendencies of the ink base at the surface. The other alternative is to use a wet assembly process, applying the MEA to the flow field plate prior to the ink drying. And still another option is to use screen printing techniques to print the electrodes right onto the surface (or subsurface) of the flow field plates followed by the printing of the membrane. This process would reduce the number of individual components and improve the electrical contact between them by removing the material boundaries

References

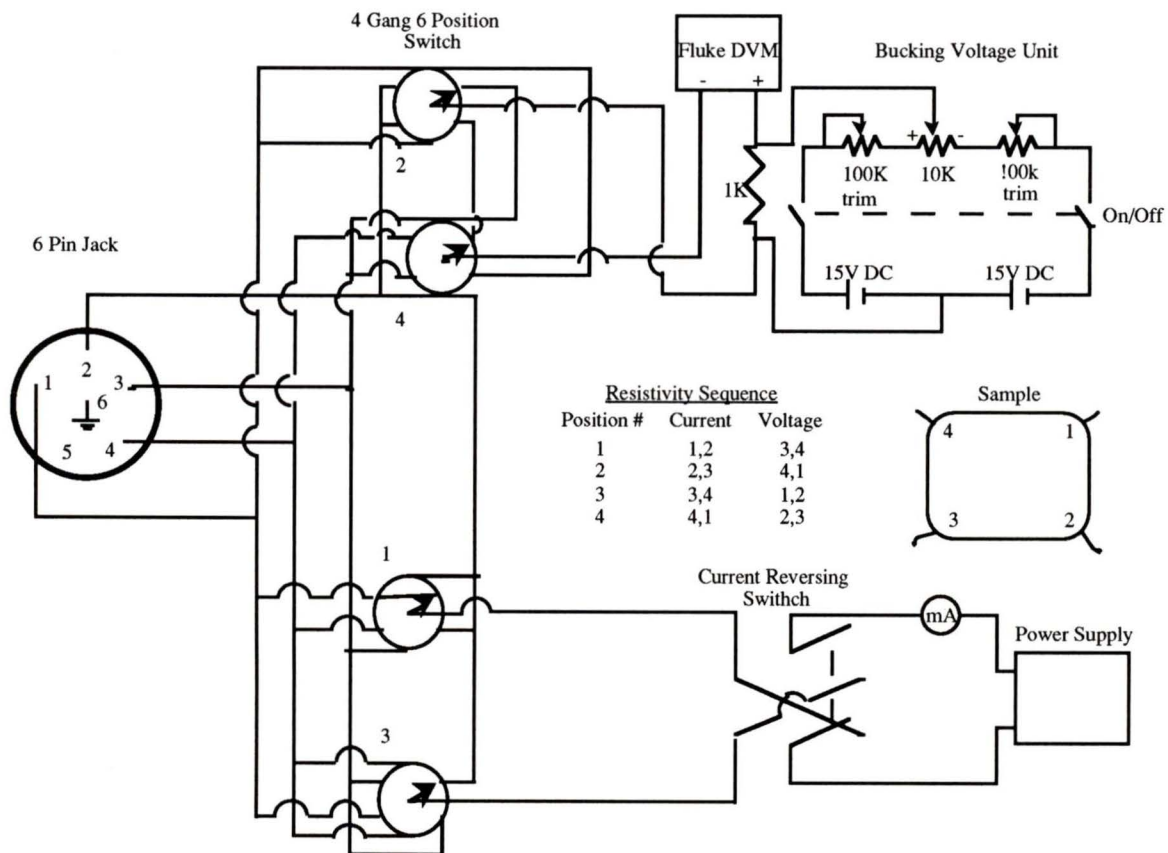
- [1] S. Kartha and P. Grimes. Fuel Cells: Energy Conversion for the Next Century. *Physics Today*, American Institute of Physics, pp. 54-61, Nov., 1994.
- [2] R.L. Borup and N.E. Vanderbough. Design and Testing Criteria for Bipolar Plate Materials for PEM Fuel Cell Applications, Material Research Society Symposium, Proceedings Volume 393, 1995.
- [3] *NGV News*, Pasha Publications, 3, No. 12, Dec. 1994.
- [4] *The Clean Fuels Report*, J.E. Sinor Consultants Inc., 6, No. 3, June 1994.
- [5] *Opening Address to the Second Working Group of the Intergovernmental Panel on Climate Change*, Deliverd by Hon. Sheila Copps, M.P., Deputy Prime Minister of Canada, Minister of the Environment, Montreal, October 16, 1995.
- [6] *Global Energy Perspectives to 2050 and Beyond*, World Energy Council, Aug. 1995.
- [7] *Clean Vehicles and Fuels for British Columbia*, B.C. Ministry of the Environment, Lands and Parks. April 1995.
- [8] Karl V. Kordesch and Guenther Simader. The Environmental Impact of the Fuel Cell Technology, *Journal of the American Chemical Society*, Spring 1995.
- [9] Leo J.M.J. Blomen and Michael N. Mugerwa (Eds.). *Fuel Cell Systems*, Plenum Press, 1993.
- [10] A. J. Appleby. Fuel Cells and Hydrogen Fuel, *International Journal of Hydrogen Energy*, Vol.19, No. 2, pp. 175-180, 1994.
- [11] John Ross, Clare Romano, and Tim Ross. *The Complete Printmaker*. Round Table Press, 1990.
- [12] John Stephens. *Screen Process Printing*. Blueprint Publishing Ltd., 1987.

- [13] Tim Mara. *The Thames and Hudson Manual of Screen Printing*. Thames and Hudson, 1979.
- [14] M.T. Kortschot and R.T. Woodhams. Computer Simulation of the Electrical Conductivity of Polymer Composites Containing Metallic Fillers. *Polymer Composites*, Vol. 9, No. 1, February, 1988.
- [15] J. Gurland. *Trans. Met. Soc. AIME.*, 236, 642 (1966).
- [16] D. Stauffer and A Aharony. *Introduction to Percolation Theory*. Taylor and Francis, 1992.
- [17] Discussion with Keith Prater of Ballard Power Systems, May 30 1996.
- [18] Dr. David Scott. Private Communication. Exergy Analysis and Energy Systems, University of Victoria, Nov 12 1995.
- [19] D.S. Scott and W. Hafele. The Coming Hydrogen Age: Preventing World Climatic Disruption. *International Journal of Hydrogen Energy*, Vol. 15, No. 10, pp 727-737, Pergammon Press, 1990.
- [20] P.F. Howard. Ballard PEM Fuel Cell Powered ZEV Bus. Internal Publication. 1993.
- [21] Technical publication on Calgraph. Published by Polycarbon Inc. 1995.
- [22] Tina Scarpelli. Private Communication. Autotype International representative. 1-800-323-0632. September 26, 1996.
- [23] Ian: Chemistry Department. Private Communication. Murakami 745 Monterey Pass Road, Monterey Park, California, 91754 USA (213) 980-0662. January 17, 1997.
- [24] Phillips Research Reports, Vol. 13, No.1, February 1958.
- [25] David Leboe. An Analysis of Ohmic Contact Losses in a Fuel Cell Stack, NGFT Internal Publication, University of Victoria, Sept 1996.
- [26] Joel Ronne. Cost Reductions of Bi-Polar Plates for SPFCs., NGFT Internal Publication, University of Victoria, May 1996.

- [27] Zuomin Dong. Invention Memo: Screen Printing as a Manufacturing Technique for Bi-polar Plates, NGFT Internal Publication, University of Victoria, Jan 1996.

Appendix A

Van der Pauw Resistivity Circuitry Layout



VITA

Surname: Perry
Given Names: Martin Leslie
Place of Birth: Moose Jaw, Saskatchewan
Date of Birth: 66/09/27

Educational Institutions Attended

University of Victoria	1995 to 1997
Royal Military College of Canada	1985 to 1989

Degrees Awarded

M.A. Sc.	University of Victoria	1997
B.Eng	Royal Military College of Canada	1989

Partial Copyright License

I hereby grant the right to lend my thesis to users of the University of Victoria Library, and to make single copies only for such users or in response to a request from the Library of any other university, or similar institution, on its behalf for one of its users. I further agree that permission for extensive copying for scholarly purposes may be granted by me or a member of the University designated by me. It is understood that copying or publication of this thesis for financial gain shall not be allowed without my written permission.

Title of Thesis: Screen Printing of Fuel and Oxidant Delivery Plates: A Low Cost Manufacturing Alternative

Author:


(Signature)

MARTIN LESLIE PERRY
(Name in Block Letters)

June 15, 1997
(Date)